

Time-dependent models of two-phase accretion discs around black holes

M. Mayer¹ & J. E. Pringle

Institute of Astronomy, Madingley Road, Cambridge CB30HA, UK

¹ *E-Mail: mm@ast.cam.ac.uk*

7 February 2020

ABSTRACT

We present time-dependent simulations of a two-phase accretion flow around a black hole. The accretion flow initially is composed of an optically thick and cool disc close to the mid-plane, while on top and below the disc there is a hot and optically thin corona. We consider several interaction mechanisms as heating of the disc by the corona and Compton cooling of the corona by the soft photons of the disc. Mass and energy can be exchanged between the disc and the corona due to thermal conduction. For the course of this more exploratory work, we limit ourselves to one particular model for a stellar mass black hole accreting at a low accretion rate. We confirm earlier both theoretical and observational results which show that at low accretion rates the disc close to the black hole cannot survive and is evaporated. Given the framework of this model, we now can follow through this phase of disc evaporation time dependently.

Key words: black hole physics – galaxies: jets – X-Rays: binaries.

1 INTRODUCTION

X-Ray spectral observations of accretion powered black holes in binary systems show that there are at least two spectral components present. The lower energy, thermal component is usually attributed to the geometrically thin but optically thick disc, which emits as a black-body or modified black-body (for the latest spectral model, BHSPEC, see Davis et al. 2005; Davis & Hubeny 2006). The higher energy, power-law component reflects the presence of a possibly geometrically thick but optically thin, hot corona. The relative importance of these components changes with time, especially during periods of strong variability when these sources undergo outbursts. If the power-law component dominates, the state is called low/hard (LH) state, while if the black-body dominates the state is called high/soft (HS) state. The nomenclature 'hard/soft' reflects the shape of the spectrum, while 'high/low' reflects the presumed accretion rate in these states. For a review on spectral states, see McClintock & Remillard (2004).

In general this picture holds for high-mass black holes, i.e. AGN (active galactic nuclei), as well. However the low-mass black holes, i.e. X-Ray Binaries, are the best studied objects with regards to the temporal behaviour. There the timescale for outbursts is on the order of weeks to months and years, while in AGN it is much longer. Hence theoretical models of accretion flows around black holes concerning the long-term stability properties are observationally best tested against X-Ray Binaries.

Many authors have addressed the thermal and physical states of the accretion flow in these systems. Much of the work has concentrated on what is required of the thermal and physical states of

the accretion flow in order to reproduce the X-ray spectra. In these papers, the system is usually assumed to be in a steady configuration, and the effort is devoted to computation of the resulting spectrum. There has also been consideration given to physical and thermal interactions between the proposed cool (disc) and hot (corona) plasmas, and it is these considerations which have the strongest bearing on the time-dependent behaviour of the flow. We briefly discuss some of this work.

Eardley et al. (1975) and Shapiro et al. (1976) introduced the concept of a two-phase accretion model. Their disc consists of an inner, hot, optically thin and geometrically thick corona, and an outer, standard, optically thick, but geometrically thin, disc. The plasma in the inner parts of the corona is a two-temperature plasma, where electrons and ions interact via Coulomb collisions. The main aim of the model was to provide an explanation of the spectrum of Cyg X-1.

Wandel & Urry (1991) and Wandel & Liang (1991) present models for spectra of Seyfert galaxies given three different underlying assumptions on the flow geometry. They discuss a "sandwich" geometry where the corona and the disc literally form a sandwich. Corona and disc are either separated radially as in Shapiro et al. (1976) or vertically. Models similar to Wandel & Liang (1991) were developed by Haardt & Maraschi (1991, 1993).

While these models were mostly concerned with the explanation of the observed spectra of the corresponding object, others considered the structural properties of these two-phase discs and the interactions between the phases.

Zycki et al. (1995) and Witt et al. (1997) present a two-phase accretion disc model where the two phases interact by Compton

cooling of the corona by soft photons and the disc and heating of the disc by illumination of the corona, respectively. They carry out an extensive parameter study of their model, and also include the effects of mass and energy loss to a wind.

Begelman & McKee (1990) examine effects of thermal conduction on two-phase media. They consider the thermal interaction of the hot and cold phases under isobaric conditions and develop criteria to determine which of the the hot or cold phase shrinks or grows.

Róžańska & Czerny (2000a) discuss radiative and conductive equilibrium for two-phase accretion disc models. They find stability/instability strongly dependent on the assumed coronal heating mechanism. In a later paper (Róžańska & Czerny 2000b) they consider mass loss/gain of both phases due to thermal conduction for stationary accretion disc models following the considerations of Begelman & McKee (1990).

Dullemond (1999) presents an semi-analytic model of disc evaporation by thermal conduction. His model is based on Meyer & Meyer-Hofmeister (1994). He calculates the detailed structure of the transition layer between disc and corona for an one-temperature corona. In order to dissolve the disc, he needs a large evaporation rate which only can be achieved if the conductive length scale is larger than the radius, so that radial thermal conduction enters the problem. He gives caveats and questions to what extent this type of accretion flow can be represented in a 1D model.

One important point in all two-phase models discussed above is how to determine the relative amounts of luminosity produced in each of the two phases. Most authors simply introduce a parameter which predetermines the fraction of luminosity produced or the fraction of accretion rate in each phase. Nakamura & Osaki (1993) assume viscous heating to operate in both the hot corona and cool disc. Given their constraints on the scaleheight of both parts, they find that most of the heat is produced in the corona. Some (e.g. Zycki et al. 1995) constrain this important parameter through some boundary conditions at the interface between corona and disc. All of these models however assume a stationary accretion flow.

It was realised fairly early that accretion in a standard optically thick disc around a black hole is viscously unstable at near-Eddington accretion rates (Lightman & Eardley 1974). Then electron scattering renders the accretion flow unstable. Abramowicz et al. (1988) discovered that in these circumstances the radial advection of energy cannot be neglected. They dubbed such discs ‘slim discs’ and found that these instabilities are stabilised by radial advection of energy. The name comes from the fact that the ratio of disc scale-height to radial distance, H/R , is close to unity (thermal energy close to kinetic energy), so that the usual ‘thin disc’ approximation is at best marginally applicable. These accretion flows are optically thick ADAFs (advection dominated accretion flow). These flows are applicable to the high/soft state.

A similar picture holds for optically thin accretion flows. Narayan & Yi (1995) and Ichimaru (1977) proposed an optically thin counterpart to the optically thick ADAF. They consider an optically thin disc, i.e. corona, close to the black hole and an standard optically thick disc further out. Their model is applicable to lower accretion rates or the so-called low/hard state. The exact transition rate from the optically thin ADAF to the optically thick disc is not predicted by these models, but is determined to match the observations.

Many of the observed black hole accretion discs show state transitions, i.e. transitions from the high/soft to the low/hard state and vice versa (McClintock & Remillard 2004). The spectrum changes from very soft and black-body dominated (attributed to

the disc) to a hard, power law dominated spectrum (attributed to the corona). These changes appear to reflect changes in the accretion rate and flow geometry as discussed by Esin et al. (1997).

In this paper we introduce the various physical concepts which are required in order to determine the time-dependence of such accretion flows. Many of the physical properties of such flows are not well-defined and it is necessary to make many simplifying assumptions along the way. We shall need to consider three possible disc states, when the disc is a standard disc with little or no corona, when the disc has a sizeable corona, and when the disc evaporates altogether and there is only a corona present. We also need to determine how the accretion flow transitions from one of these states to another. For example, if the disc is truncated at low accretion rates and the inner flow is filled with a hot corona, then we need to determine the transition radius below which the disc cannot exist any more. Thus we need to introduce a time-dependent two-phase model for black hole accretion discs, where mass can be exchanged between the two phases owing to thermal conduction.

Because the modelling of all these processes is computationally demanding (apart from all the physical complications this comes about basically because we need to follow thermal timescales in the inner hot disc for several viscous timescales of the outer cool disc), we present here just one example of a time-dependent computation. We take as an initial condition a steady-state flow where the hot and optically thick corona sandwiches a cool and geometrically thin disc for which the accretion rates in each component are predetermined. This is similar to some of the models derived in the literature of the kind invoked to explain the spectral characteristics of these objects (see above). We then fix the total accretion rate at the outer boundary and allow the disc to evolve, permitting radial viscous evolution of both the disc and coronal components, and well as thermal energy and mass flow between them.

We give a detailed description of the physical assumptions we make to describe model in Sect. 2. These assumptions of necessity over-simplify the problem and are certainly not unique, they should however give a reasonable indication of the sort of behaviour we might expect from such discs. In Sect. 3 we discuss the relative contributions of the corona and disc to the total luminosity and we also briefly review some observational results. We then discuss the time-dependent equations for the two-phase flow in Section 4 and describe the numerical setup in Sect. 5. We describe our results in Sect. 6, discuss them in Section 7 and end with the conclusions in Sect. 8.

2 THE MODEL

We assume that at a given radius the general accretion flow consists of an optically thick but geometrically thin accretion disc which is sandwiched by a hot geometrically thick and optically thin corona above and below. In the following we refer to these parts of the flow as disc and corona, respectively. Note that at any radius, it may be that either the disc, or the corona, is not present.

We describe the physics of the disc in Section 2.1, the corona in Sect. 2.2 and the transition layer in 2.3. The disc or the corona might cease to exist if either of them is evaporated, we discuss the treatment of these cases in Section 2.4.

2.1 The disc

We model the disc as a standard accretion disc in the so-called one-zone approximation. Hence the density ρ_d and temperature T_d just represent some average values at a given radius R . Taking constant density, the equation of hydrostatic equilibrium gives a pressure distribution of the form

$$P_d(z) = P_d(0) - \frac{1}{2} \rho_d \Omega_d^2 z^2, \quad (1)$$

where Ω_d is the rotational frequency of the disc which we assume to be Keplerian, i.e. $\Omega_d = \sqrt{GM/R^3}$. $P_d(z)$ is the pressure at a height z above the midplane. The pressure in the midplane, which we also take to be the representative pressure for the disc, contains contributions of gas and radiation pressure,

$$P_d \equiv P_d(0) = \rho_d \frac{kT_d}{\mu m_p} + \frac{4\sigma}{3c} T_d^4, \quad (2)$$

where we consider a fully ionised, solar metallicity gas. Thus we set the mean molecular weight $\mu = 0.6$. Here k is the Boltzmann constant and σ is the Stefan-Boltzmann constant.

When the disc is optically thick, the disc radiates as a black body and we can treat the radiative transfer in the diffusion approximation, i.e. we write for the one-sided radiative losses in the disc

$$\Lambda_d^- = \frac{4\sigma}{3\kappa_R \rho_d H_d} T_d^4, \quad (3)$$

where κ_R is the Rosseland mean of the opacity. We use the tabulated values of the OPAL opacity project (Rogers & Iglesias 1992; Iglesias & Rogers 1996) for the solar composition of Grevesse & Noels (1993). We use the $X = 0.7$ set of their opacity tables (X is the hydrogen mass fraction of the matter) for solar metallicity ($Z = 0.02$).

Energy in the disc is generated by viscosity ν . We use the parametrisation by Shakura & Sunyaev (1973), i.e.

$$\nu = \alpha c_s H, \quad (4)$$

where α is the viscosity parameter (typically smaller than unity, we use $\alpha = 0.1$), $c_s \approx \sqrt{P/\rho}$ the sound speed in the medium and H the scale-height. The viscosity produces a torque

$$G_d = -\frac{3}{2} \pi \nu_d \rho_d H_d R^2 \Omega_d, \quad (5)$$

which gives rise to viscous dissipation

$$Q_d^+ = \frac{9}{8} \nu_d \rho_d H_d \Omega_d^2. \quad (6)$$

In both cases we made use of the fact that the disc rotates at the Keplerian speed, i.e. $\partial(\log \Omega_d)/\partial(\log R) = -3/2$.

2.2 The corona

As for the disc, we take again density within the corona constant and equal to some representative value. The pressure distribution in the corona at height $x = z - H_d$ above the disc/corona interface is given by

$$P_c(x + H_d) = P_c(H_d) - \rho_c \Omega_c^2 \left(H_d + \frac{1}{2} x \right) x, \quad (7)$$

where ρ_c is the (representative) density in the corona, x the height above the disc and H_d the height of the disc. The point where $P_c(x + H_d) = 0$ defines the thickness of the corona, i.e.

$$P_c(H_d) - \rho_c \Omega_c^2 \left(H_d + \frac{1}{2} H_c \right) H_c = 0. \quad (8)$$

We set $P_c(H_d) = P_c$ to determine the representative pressure in the corona, and note that $P_c \neq P_d$. Typically in the corona the representative electron and ion temperatures ($T_{e,c}$ and $T_{p,c}$) are not equal. The corona is optically thin, and so we take the representative values of pressure, density and temperature in the corona to be related by

$$P_c = \rho_c \frac{k (T_{p,c} + T_{e,c})}{2 \mu m_p}. \quad (9)$$

Note the factor 2 in the denominator of eq. (9). It ensures that for a one-temperature plasma ($T_{p,c} = T_{e,c}$) the correct value for the gas pressure is recovered (cf. eq. 2). We assume a pure hydrogen plasma for the corona (number density of electrons equals number density of protons). An extension to non-hydrogen plasmas involves factors of a few percent in (9). Given the other approximations made here, not least the simplification of the one-zone model, we can safely neglect these factors for the purposes of this paper.

We use the same viscosity prescription in the corona as for the disc (see eq. 4), adjusted to the corresponding values in the corona. The torque in the corona is given by

$$G_c = -\frac{3}{2} \pi \nu_c \rho_c H_c R^2 \Omega_c, \quad (10)$$

and the heating rate in the corona is

$$Q_c^+ = \frac{9}{8} \nu_c \rho_c H_c \Omega_c^2. \quad (11)$$

The scaleheight of the corona may be comparable to the radial distance from the black hole, i.e. $H_c/R \approx 1$. Then the coronal flow is pressure supported and deviates from Keplerian rotation. In the course of this paper however we keep the assumption of Keplerian rotation for the corona as well. As long as H_c/R does not greatly exceed unity, there are only factors of about two involved. They are however comparable to the likely errors we make in the vertical averaging and thus we neglect them.

The heating in the corona is distributed onto the electrons and protons. The fraction of heat going into electrons and protons is not very well known. Gruzinov (1998) shows that if the magnetic fields are near to equipartition, high radiative efficiency is achieved and most of the viscous heat goes into the electrons, while for low magnetic fields the heat goes mainly in the ions and low radiative efficiency, as assumed by ADAF models can be reproduced. Quataert (1998), on the other hand, argues that there is damping at the protons Larmor radius and hence most of the viscous energy heats the protons. This picture has been reconciled by Quataert & Gruzinov (1999), who show that for equipartition magnetic fields most of the energy heats the electrons, while for a small magnetic field the energy primarily goes into the ions. They find a transition for $\beta_B = 5$ to $\beta_B = 100$, where β_B is the ratio of gas to magnetic pressure. The uncertainty then is introduced by uncertainties how Alfvén waves are converted into whistlers on the protons Larmor radius. In the light of this discussion, we define our "fiducial" heating model for the corona by heating ions and electrons according to their partial pressure, $P_{p,c}$ and $P_{e,c}$, i.e. we take

$$Q_{p,c}^+ = Q_c^+ \frac{P_{p,c}}{P} \quad (12)$$

and

$$Q_{e,c}^+ = Q_c^+ \frac{P_{e,c}}{P}, \quad (13)$$

respectively. This, together with the Coulomb collisions, intro-

duced below, leads to a preferred ion heating for a two-temperature plasma, and an equal share for a one-temperature plasma.

Electrons and protons are coupled through Coulomb collisions. They transfer heat from the protons to the electrons at a rate Q_{ep} . We take the rate as calculated by Stepney & Guilbert (1983).

The electrons cool radiatively by bremsstrahlung and other cooling processes (atomic line cooling etc.). While there are cooling rates for different metallicities and physical conditions available in the literature (e.g. Sutherland & Dopita 1993) we limit ourselves here solely to electron-proton bremsstrahlung. We use the recently recalculated rate $\Lambda_{\text{brems}}(T_{e,c}, T_{p,c})$ by Mayer (2007). The recalculation accommodates the previously overlooked fact that for a two-temperature plasma the protons can contribute a significant fraction of the bremsstrahlung due to their plasma speed. For proton temperatures in excess of $T_{p,c} > m_p/m_e T_{e,c}$ the proton thermal speed is larger than that of the electron and correspondingly most of the bremsstrahlung is produced by the deceleration of the proton rather than the electron. This calculation however strictly is only valid for the non-relativistic regime, although it could be generalised to include this if required.

Soft photons from the disc cool/heat the corona by Compton scattering at a rate (e.g. Rybicki & Lightman 1979)

$$\Lambda_{e,c,C} = \Lambda_d \max(\tau_{es}, \tau_{es}^2) \left[\max(4\theta_e, 16\theta_e^2) - \frac{4kT_{\text{eff},d}}{m_e c^2} \right], \quad (14)$$

where Λ_d is the soft photon source (see eq. 3), $\tau_{es} = \kappa_{es} \rho_c H_c$ the electron scattering optical depth ($\kappa_{es} = 0.3 \text{ cm}^2 \text{ g}^{-1}$), $\theta_e = kT_{e,c}/(m_e c^2)$ and $T_{\text{eff},d}$ the effective temperature of the disc. Both an Compton thick corona ($\tau_{es} > 1$ or slightly relativistic electrons ($\theta_e > 1/4$) lead to a strong increase in the cooling rate and therefore try to keep the electron temperature at $\theta_e \approx 1/4$, i.e. $T_e \approx 1.5 \times 10^9 \text{ K}$, or lower. The first term in the square brackets correspond to Compton cooling, while the second reflects Compton heating. Note that the use of the effective temperature in (14) for Compton heating is valid only if the disc emission dominates. Then the inverse Compton temperature equals the effective temperature of the disc. In general, $T_{\text{eff},d}$ should be replaced by a term proportional to the flux weighted energy per photon (e.g. Reynolds & Wilms 2000). For the cases presented in this paper, the electron temperature in the corona is always larger than 10^8 K , i.e. Compton heating never plays an important role.

For the corona we assume a local two-stream radiation field, i.e. half of the radiation (Bremsstrahlung and Compton radiation) is directed upwards and leaves the system, while the other half is directed downwards. If the disc exists, this part of the radiation field heats the disc at a rate

$$Q_{\text{heat},d} = \frac{1-a}{2} (\Lambda_{e,c,C} + \Lambda_{\text{brems}}(T_{e,c}, T_{p,c})), \quad (15)$$

where a is the albedo of the disc. For $a = 0$ all radiation is absorbed while $a = 1$ corresponds to a perfect reflector. Haardt & Maraschi (1991) estimate the albedo to be between 0.1 and 0.2 by Monte Carlo simulations. Without any significant loss of accuracy, we set the albedo $a = 0$, so that all the radiation impinging on the disc (if it exists) is assumed to be absorbed.

2.3 The transition layer

We now need to consider the structure within the transition layer between the disc and the corona. We first assume that the pressure across the transition zone is constant, i.e. we set

$$P = P_d(H_d) = P_c(H_d) \quad (16)$$

and hence in the transition layer of width ΔH (We essentially need and assume $\Delta H \ll (H_d, H_c)$) only density and temperature vary.

In the transition layer heat is exchanged by thermal conduction (see Sect. B). This process leads to mass and energy exchange between disc and corona by condensation and evaporation. The amount of mass flowing through the transition layer is assumed to be sufficiently slow that it does not affect the hydrostatic equilibrium and sufficiently fast that it can be treated as a stationary, i.e. time-independent, process, which only depends on the actual physical state of the corona and disc.

We write for the energy transport in the transition layer, following Begelman & McKee (1990)

$$\frac{d}{dz} \left(\dot{m}_z \frac{5}{2} \frac{k(T_p + T_e)}{2\mu m_p} + q_{\text{cond}} \right) = q^+ - q^-, \quad (17)$$

where \dot{m}_z is the mass flow rate per (disc) surface area, q_{cond} is the conductive flux of heat given in (B4) and q^+ and q^- are volume heating and cooling rates as opposed to the vertically integrated heating and cooling rates used above. If $\dot{m}_z > 0$, then the disc evaporates into the corona, and if $\dot{m}_z < 0$ the corona condenses into the disc.

The characteristic length scale for eq. (17) is the so-called Field length (Field 1965), i.e.

$$\lambda_F = \left(\frac{\kappa_{\text{cond}} T}{\max(q^+, q^-)} \right)^{\frac{1}{2}} \quad (18)$$

It can be shown that for a one-temperature plasma a stationary corona (accretion rate independent of radius), where the viscous heating dominates, leads to a ratio between the Field length and the height of the corona of

$$\frac{\lambda_F}{H_c} = \left(\frac{6\pi\kappa_{\text{cond}}(T)T}{\dot{M}\Omega\sqrt{kT/(\mu m_p)}} \right)^{\frac{1}{2}} \quad (19)$$

If we assume that the luminosity L of the disc corresponds to the accretion rate \dot{M} via $L = \eta \dot{M} c^2$, where c is the speed of light and $\eta = 1/12$ the efficiency of converting rest mass into energy, we can scale the accretion rate and luminosity in terms of the Eddington luminosity and accretion rate L_{Edd} and \dot{M}_{Edd} . We get for the ratio

$$\frac{\lambda_F}{H_c} = 1.7 \cdot 10^{-3} \left(\frac{R}{R_{\text{S}}} \right)^{\frac{3}{4}} \left(\frac{\dot{M}}{\dot{M}_{\text{Edd}}} \right)^{-\frac{1}{2}} \left(\frac{T_e}{10^9 \text{ K}} \right)^{\frac{3}{2}} \left(\frac{T_e}{T_p} \right)^{\frac{1}{4}} \quad (20)$$

Note that the result is independent of the mass. For $R = 300 R_{\text{S}}$ and $T_e = T_p = 10^9 \text{ K}$ and $M = 10^{-3} M_{\text{Edd}}$ we get $\lambda_F/H_c \approx 0.12$. Hence the assumption is justified, at least with respect to the corona.

The volume heating rate of the disc can be reduced to an expression only containing pressure and rotation frequency by using the hydrostatic equilibrium (eq. 1) and the dissipation rate (6) to get

$$q_d^+ \equiv \frac{Q_d^+}{H_d} = \frac{9}{8} \alpha P_d \Omega \sqrt{2}. \quad (21)$$

and similarly the dissipation rate of the corona (using eq. 7 and 11)

$$q_c^+ \equiv \frac{Q_c^+}{H_c} = \frac{9}{8} \alpha P_c \Omega \sqrt{\frac{H_c}{H_d + \frac{1}{2} H_c}}. \quad (22)$$

Note that for a thick corona ($H_c \gg H_d$) the volume heating rates show the same proportionalities ($\propto \alpha P \Omega$). For a thin corona on top of a thick disc ($H_c \ll H_d$), the volume heating rate is reduced by a factor $(H_c/H_d)^{\frac{1}{2}}$.

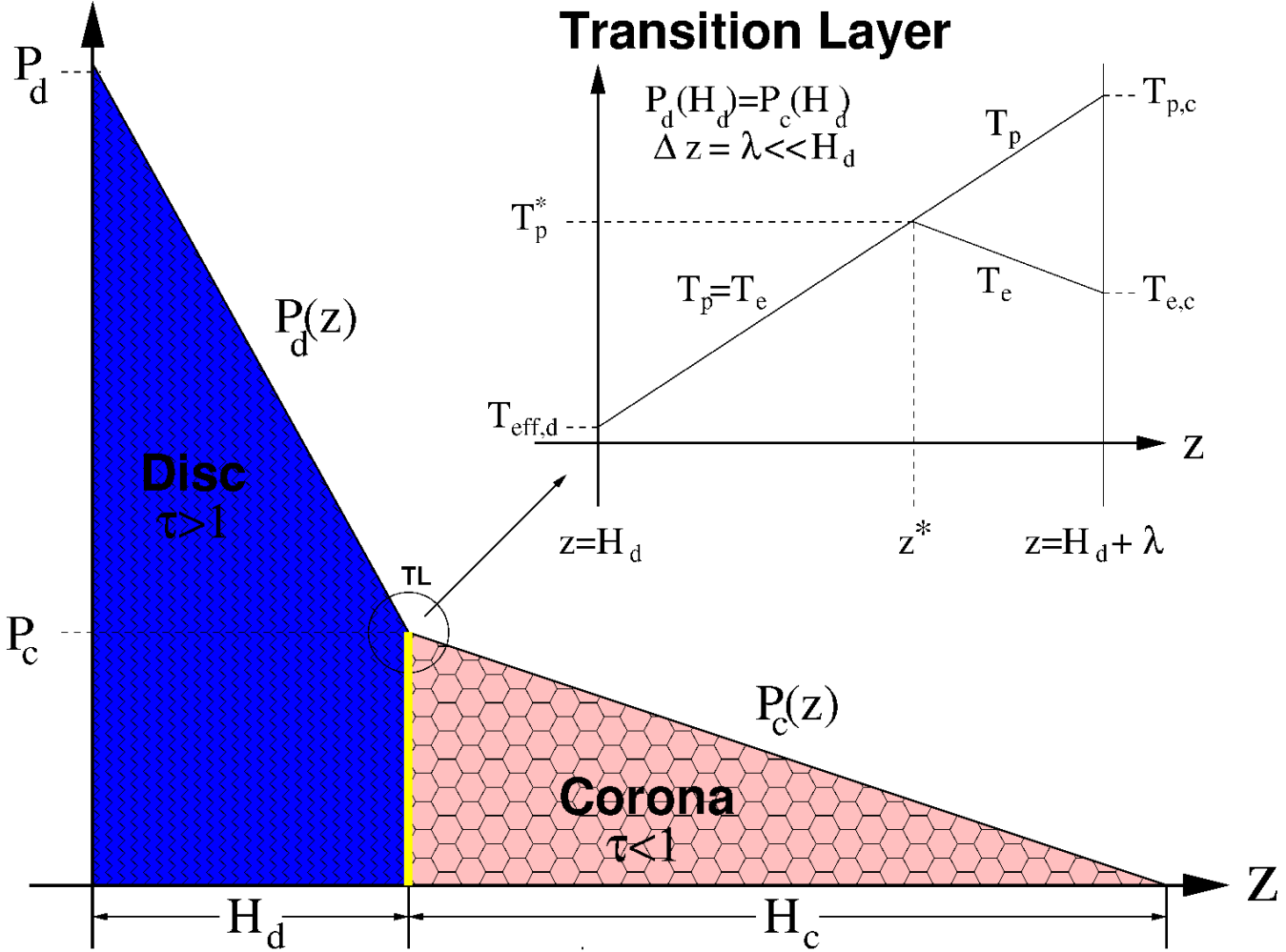


Figure 1. Schematic picture of our disc-corona sandwich, starting from the midplane ($z=0$) upwards. The disc has a half-thickness of H_d , while the coronal layer has a thickness of H_c . The average pressure in the disc is approximated by the pressure in the midplane, P_d and the pressure in the corona by the pressure at the base of it, P_c . For simplicity we plot the pressure as a linear function of the height. At the disc-corona interface the pressure at the base of the corona and the top of the disc is matched smoothly. We indicate the presumed temperature structure in the thin transition layer (TL) in the small inset. The pressure there is constant, but the temperature changes from the effective temperature of the disc $T_{\text{eff},d}$ to the electron and proton temperature of the corona ($T_{p,c}$ and $T_{e,c}$), including a (possible) transition to a two-temperature plasma, if the ion temperature exceeds T_p^* . Note that the length and pressure values are not to scale.

The cooling terms can be calculated accordingly. For Compton cooling we get the volume cooling rate from (14)

$$q_{c,C}^- \equiv \frac{\Lambda_{c,e,C}}{H_c} = \kappa_{\text{es}} \rho \Lambda_d \left(\max(4\theta_e, 16\theta_e^2) - \frac{4kT_{\text{eff},d}}{m_e c^2} \right), \quad (23)$$

where we assumed a Compton thin transition layer. Given the geometrical thinness of the layer (see eq. 20) compared to the corona, this approach is justified. The volume cooling rate (23) is strictly valid only for an entirely optically thin corona.

We now need to solve (17). We follow Begelman & McKee (1990) and Różańska & Czerny (2000b) and multiply by q_{cond} and integrate over the transition layer to get

$$\begin{aligned} & \int_{H_d}^{H_d + \lambda_F} \frac{d}{dz} \left(\dot{m}_z \frac{5}{2} \frac{k(T_p + T_e)}{2\mu m_p} \right) q_{\text{cond}} dz \\ & + \frac{1}{2} \left(q_{\text{cond}} (H_d + \lambda_F)^2 - q_{\text{cond}} (H_d)^2 \right) = \int_{H_d}^{H_d + \lambda_F} (q_{\text{TL}}^+ - q_{\text{TL}}^-) q_{\text{cond}} dz \end{aligned} \quad (24)$$

The conductive flux at the boundaries of the transition layer

is zero. If we now define the Field length using the result of Różańska & Czerny (2000b), then we get

$$\lambda_F \approx \frac{\int_{H_d}^{H_d + \lambda_F} q_{\text{cond}} dz}{\left| \int_{H_d}^{H_d + \lambda_F} (q_{\text{TL}}^+ - q_{\text{TL}}^-) q_{\text{cond}} dz \right|^{\frac{1}{2}}}. \quad (25)$$

Since the conductive flux contains a temperature gradient, the integrals over the width of the transition layer in (25) can be transformed in an integral over the corresponding electron and proton temperatures. Note that this definition of the Field length differs from the one in (18), but for the relevant limiting case (coronal electron and proton temperature much larger than the disc values and either heating or cooling dominating the other) they are equivalent. For heating equals cooling the Field length formally goes to infinity, but then physically there is no mass flux due to conduction either.

We are only interested in an average mass flux in the transition layer. Thus we take $\dot{m}_z = \text{const.}$ and hence can put \dot{m}_z outside the integral on the right hand side of (24). The knowledge of the Field

length (25) allows us to estimate an average conductive flux by setting $\partial T / \partial z \approx T / \lambda_F$ where we assume that the coronal electron and proton temperature is much larger than the disc temperature. We finally find an estimate for the condensation/evaporation rate \dot{m}_z to

$$\dot{m}_z = \frac{\int_{T_{\text{eff},d}}^{T_{e,c}, T_{p,c}} (q_{\text{TL}}^+ - q_{\text{TL}}^-) \kappa_{\text{cond}} (dT_e + \zeta_{\text{ep}} dT_p) - 2 \frac{2 \mu m_p}{k (T_{e,c} + T_{p,c})}}{\left| \int_{T_{\text{eff},d}}^{T_{e,c}, T_{p,c}} (q_{\text{TL}}^+ - q_{\text{TL}}^-) \kappa_{\text{cond}} (dT_e + \zeta_{\text{ep}} dT_p) \right|^{\frac{1}{2}}} \frac{2}{5}, \quad (26)$$

where we set $\zeta_{\text{ep}} = m_e / m_p$. For the heating we use the viscous volume heating rate (22), while for the cooling we use the volume rate for Compton cooling (23) and Bremsstrahlung from $\Lambda_{\text{brems}}(T_{e,c}, T_{p,c})$, which we divide by the corona scale-height to get the volume cooling rate, accordingly.

The sign of \dot{m}_z crucially depends on the net effect of the heating and cooling balance in the transition layer. If the cooling dominates the heating in the transition layer, then hot matter from the corona condenses into the disc ($\dot{m}_z < 0$). If the heating dominates, disk matter evaporates into the corona ($\dot{m}_z > 0$).

We show a schematic picture of the disc-corona sandwich including the transition layer temperature structure in Fig. 1. In the inset we show the assumed temperature structure of the transition layer. The proton temperature is assumed to rise monotonically from the photosphere, i.e. the effective temperature of the disc, to the coronal value. At some critical value T_p^* however the proton-electron coupling becomes very weak. Then electrons and protons start to have different temperatures. We set this critical temperature to $T_p^* = 3 \cdot 10^9$ K. For the evaluation of \dot{m}_z according to eq. (26) we need to take this consideration into account. For a one-temperature corona, we safely can neglect the integration over T_p , since it only enters with a factor of m_e / m_p . For a two-temperature corona, we need to integrate from $T_{\text{eff},d}$ to $T_p = T_e = T_p^*$ and then until $T_{p,c}$ and $T_{e,c}$, respectively.

We tabulate parts of the integral for selected values of $T_{p,c}$, $T_{e,c}$ and $T_{\text{eff},d}$ and use interpolations in these three variables to calculate \dot{m}_z in order to save computational time.

2.4 Truncation

At some point in the evolution of the disc-corona sandwich the disc or the corona can cease to exist at some radius. The determination of the exact transition to the corona or disc only state however is not straightforward. We discuss the two cases below.

2.4.1 Disc truncation

Here we take the simple approach that whenever the surface density of the disc falls below a fraction of the surface density of the corona at that point, we assume the disc does not exist any more. We assume the disc ceases to exist if the surface density of the disc is smaller than 80 per cent of the coronal surface density. The disc is "reborn" if the disc surface density exceeds 90 per cent of the coronal surface density.

The corona a priori never becomes opaque to absorption and does not reach values to become optically thick to electron scattering either. Hence our disc evaporation criterion approximately coincides with the point where the electron scattering optical depth of the disc, $\tau_{\text{es}} = \kappa_{\text{es}} \Sigma_c$ becomes lower than unity. Then our assumption of optical thick radiative transfer (eq. 3) cannot be used any more for similar reasons and different methods need to be used.

If the electron scattering optical depth of the disc becomes

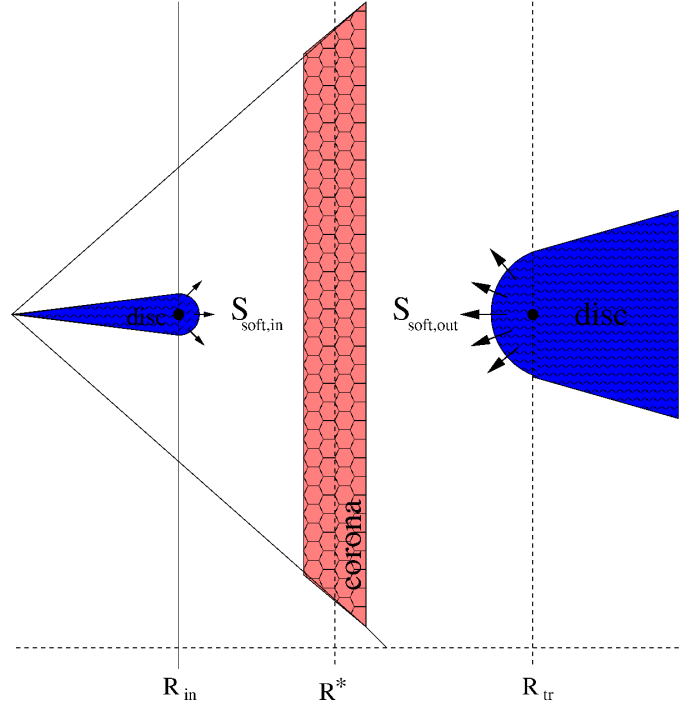


Figure 2. Schematic picture of the truncated disc. The region between R_{in} and R_{out} is filled with hot coronal gas only (a sample coronal column at R^* is shown in pink), while the outer and inner parts still consist of an optically thick disc with a hot corona above and below. The coronal gas in the truncated region can only be Compton cooled by soft photons supplied by the outer and inner disc (shown in blue).

lower than unity, then the high-energy radiation of the corona cannot be scattered or absorbed either and the heating (15) cannot operate any more. The disc becomes translucent. To which extent there can be an optically thin, but cool layer of gas, is not obvious. In the course of this paper we simply assume that it cannot exist and these parts of the accretion flow are completely filled with hot coronal gas.

The truncation criterion used in this paper is somewhat unrealistic, since even long before the disc becomes optically thin to electron scattering, it is optically thin to absorption and then it cannot thermalize internally produced or incoming radiation. The disc will heat up under such conditions and eventually become part of the corona. Our assumption however still can be used, since the actual transition from a disc-corona sandwich to a corona only state takes place over a very small radial distance. Assuming a more relaxed condition (i.e. truncate the disc if its surface density is smaller than 10^2 times the coronal surface density), the results are still very similar.

The hot corona-only phase in the middle has to be cooled by soft photons coming from the disc further out and/or, if it still exists, from the inner disc as well. We show the situation schematically in Fig. 2. The outer disc supplies a total rate of soft photons of

$$S_{\text{soft,out}} = 4\pi \int_{R_{\text{tr}}}^{\infty} \sigma T_{\text{eff},d}^4 R dR \quad (27)$$

For convenience we integrate to ∞ , i.e. the outer boundary of the disc, since $\sigma T_{\text{eff},d}^4 \propto R^{-3}$ and thus the integral only depends on the value of the effective temperature close to R_{tr} . At a radius $R^* < R_{\text{tr}}$, only a fraction of $f = 2\pi R^* H(R^*) / (2\pi(R_{\text{tr}} - R^*)^2)$ passes through

the corona, i.e.

$$f = \frac{R^* H(R^*)}{(R_{\text{tr}} - R^*)^2}. \quad (28)$$

On the way from R_{tr} to R^* the amount of soft photons is reduced due to scattering at radii R with $R^* < R < R_{\text{tr}}$. Because the corona is optically thin to electron scattering in vertical direction, the same holds in radial direction (since $H_c \approx R$). Hence this dilution is not very significant and we neglect it here. Since $\tau_{\text{es}} < 1$, the dilution factor, $\exp(-\tau_{\text{es}})$ is close to unity. At R^* the fraction f of the soft photon rate S_{soft} passes through the area $4\pi R^* H(R^*)$, i.e. we have the soft flux at R^*

$$F_{\text{soft,out}} = \frac{S_{\text{soft,out}}}{4\pi(R_{\text{tr}} - R^*)^2} \quad (29)$$

The electron scattering optical depth in the interval $[R^* - \Delta R/2, R^* + \Delta R/2]$ can be approximated by

$$\tau_{\text{es}}(R^*) = \kappa_{\text{es}} \rho_c (R^*) \Delta R. \quad (30)$$

We calculate the Coulomb cooling rate at R^* by multiplying by $4kT_{c,e}/(m_e c^2)$. Division by ΔR leads to the corresponding volume cooling rate and multiplication with H_c to the final cooling rate

$$\Lambda_{\text{e,c,C,out}} = \frac{S_{\text{soft,out}}}{\pi(R_{\text{tr}} - R^*)^2} \frac{kT_{c,e}}{m_e c^2} \kappa_{\text{es}} \rho_c H_c \quad (31)$$

Similar arguments hold for the Compton cooling which comes from the inner disc. Assume the inner disc ends at $R_{\text{in}} > 3R_S$, then the ratio of the Compton cooling at $R_{\text{in}} < R^* < R_{\text{tr}}$ is

$$\frac{\Lambda_{\text{e,c,C,in}}}{\Lambda_{\text{e,c,C,out}}} = \left(\frac{R_{\text{tr}} - R^*}{R^* - R_{\text{in}}} \right)^2 \frac{S_{\text{soft,in}}}{S_{\text{soft,out}}}. \quad (32)$$

The first factor on the right hand side changes from values much larger than unity for $R^* \rightarrow R_{\text{in}}$ to values much smaller than unity for $R^* \rightarrow R_{\text{tr}}$. The second term, the ratio between the soft photon rates, is proportional to $R_{\text{in}}/R_{\text{tr}}$ (Here we assumed again $T_{\text{eff,d}} \propto R^{-3}$). Hence the contribution of the soft photon flux from the inner disc is, as expected, only large close to the inner disc. For the calculation we retain this contribution and write

$$\Lambda_{\text{e,c,C,in}} = \frac{S_{\text{soft,in}}}{\pi(R^* - R_{\text{in}})^2} \frac{kT_{c,e}}{m_e c^2} \kappa_{\text{es}} \rho_c H_c. \quad (33)$$

2.4.2 Corona truncated

At some point in the evolution of the accretion flow, the cooling of the corona can exceed the heating and the scale-height of the decreases while the density increases. This is especially true for the parts of the corona further away from the centre. There cooling mechanisms in addition to those considered in this paper, like atomic cooling, make the corona thermally unstable and lead to runaway cooling. The cooling can be halted by Compton heating (cf. eq. 14 for $T_{\text{eff,d}} > T_{c,e}$). Then the coronal matter effectively becomes part of the disc. It also may be halted by the onset of radiation pressure as the optical depth to absorption approaches or maybe even exceeds unity. The non-negligible optical depth will also cause photoionisation heating, since the soft photons of the disc get absorbed by the collapsing corona. The examination to which extent photoionisation can stabilise the corona is likely to be important in some circumstances but is beyond the scope of this paper. If at some radius the corona completely collapses and becomes part of the disc, then these parts of the disc are still heated by the hard radiation coming from nearby disc annuli where the corona still exists.

3 THE RELATIVE IMPORTANCE OF THE CORONA AND THE DISC FOR THE TOTAL LUMINOSITY

To give an indication of the disc structure we are likely to be aiming at, we now estimate what fraction of the luminosity can be produced by the different parts of a disc and corona sandwich. For simplicity, to make a rough estimate, we here neglect radial advection and conductive losses/gains. The results of these estimates give a strong hint as to the radial extent of the corona and the disc, and we discuss some of the results from such considerations which are to be found in the literature.

The stationary, i.e. time-independent version of eq. (43) is

$$Q_d^+ + Q_{\text{heat,d}} = \Lambda_d^-, \quad (34)$$

and for the corona (combined for electrons and protons)

$$Q_c^+ = \Lambda_{\text{brems}} + \Lambda_{\text{e,c,C}}^-. \quad (35)$$

If the disc has an albedo a , then the corona heats the disc at a rate $Q_{\text{heat,d}} = 1/2(1-a)(\Lambda_{\text{brems}} + \Lambda_{\text{e,c,C}}^-)$. The remainder of the luminosity created in the corona escapes and equals the observable luminosity

$$L_c = \frac{1+a}{2} (\Lambda_{\text{brems}} + \Lambda_{\text{e,c,C}}^-). \quad (36)$$

The luminosity of the disc is simply $L_d = \Lambda_d^-$. The coronal luminosity can be written as $L_c = (1+a)/(1-a)Q_{\text{heat,d}}$. Hence the fraction L_c/L_d is

$$L_c/L_d = (1+a)/(1-a)Q_{\text{heat,d}}/\Lambda_d^-. \quad (37)$$

It is evident from eq. (34), that $Q_{\text{heat,d}}$ is always smaller than Λ_d^- . Thus the maximum luminosity ratio for a passively heated disc can be $L_c/L_d = (1+a)/(1-a) \approx 1.35$ where we set $a = 0.15$ (Haardt & Maraschi 1991). Such a ratio applies for a passively only heated stationary disc. In all other cases the ratio will be lower.

Coronal luminosities much larger than disc luminosities (representative for the low/hard state) can be produced in two obvious situations: either the disc is truncated and the inner accretion flow solely consists of hot, coronal gas, being cooled by soft photons from the outer disc, or we view the system along specific lines-of-sight and take into account relativistic effects.

In the case of X-Ray binaries there is mounting evidence that the disc is truncated in some states. Esin et al. (1997) gives an unified picture for black hole accretion flows. They use the accretion rate as indicator for the different states. For the low-hard and quiescent states they find a truncated disc, where the inner disc is filled with an hot coronal advection dominated accretion flow. Homan et al. (2001) and Belloni (2004) introduce HID (hardness intensity diagram) as a phenomenological tool to distinguish different states of X-Ray binaries in a unified scenario. Fender et al. (2004) include contributions from a jet in this scheme. In their low/hard state they assume a truncated disc.

Barrio et al. (2003) discuss the geometry of the accretion flow in Cyg X-1. They fit the spectra in the energy range from 3-200 keV with two models. One model utilises magnetic flares above an untruncated disc and the other assumes an truncated disc with an inner hot accretion flow. For the strong reflection in the magnetic flare case they do not find a break in the spectrum at high energies while with the weakly illuminated, truncated disc model they easily can fit the 3-200 keV spectra.

Kubota & Done (2004) discuss the very high-state geometry of XTE J1550-564. They calculate the luminosity L_d of the disc emission and show that in the very high state the luminosity is not

compatible with $L_d \propto T_d^4$, where T_d is the effective temperature of the disc. They conclude that the simplest explanation might be a smaller effective area where the disc emission is emitted, i.e. a truncated disc.

Done & Gierliński (2006) show that in XTE J1650-500 the broad iron line often attributed to extreme relativistic smearing can be well explained in the truncated disc geometry. Then the broad iron line is formed in an outflowing disc wind and the smearing is significantly reduced.

For AGN, the situation does not look that dissimilar. However observable black-body components only can be expected from the very lower-mass AGN, since only then the effective temperature is accessible to present X-Ray satellites.

Ptak et al. (2004) present observations of NGC 3398. They fail to find any signs of reflection from an optically thick disc. Thus they conclude that the disc is truncated at roughly 100-300 Schwarzschild radii. Similar conclusions are found by Starling et al. (2005) in the case of NGC 7213. Zhang & Wu (2006) use a truncated disc model to fit observations of the Seyfert galaxies NGC 5548 and NGC 4051. They find a disc truncated at 17...70 and 700 Schwarzschild radii, respectively. Models using reflection (therefore assuming an optically thick disc all the way down to the last stable orbit) however seem to fit the spectrum equally well (for NGC 4051, see Ponti et al. 2006).

4 THE TIME-DEPENDENT EQUATIONS

Having introduced the various physical considerations we require, we are now in a position to introduce the time-dependent equations for our model. For the energy equations we follow Mayer & Pringle (2006). We use the mass per unit area (i.e. the surface density Σ) and the internal energy e per unit mass in the disc and corona as independent variables (for the corona we consider the internal energy for the electrons, $e_{e,c}$ and protons, $e_{p,c}$, separately). All other variables can be determined by solving eqns. (A1), (A3) and (A4) in Appendix A.

4.1 Continuity equations and angular momentum transport

For the continuity equations we use

$$\frac{\partial \Sigma_d}{\partial t} + \frac{1}{2\pi R} \frac{\partial \dot{M}_d}{\partial R} = -\dot{m}_z, \quad (38)$$

and

$$\frac{\partial \Sigma_c}{\partial t} + \frac{1}{2\pi R} \frac{\partial \dot{M}_c}{\partial R} = \dot{m}_z, \quad (39)$$

where Σ_d and Σ_c are the surface density and \dot{M}_d and \dot{M}_c the accretion rates in the disc and corona, respectively. \dot{m}_z is the mass transfer due to thermal conduction (see eq. 26). $\dot{m}_z > 0$ corresponds to disc evaporation, while $\dot{m}_z < 0$ corresponds to the condensation of the corona into the disc.

We calculate the accretion rates from the angular momentum transport equations where we assume an additional source/sink term for mass gain/loss. In combination with the continuity equations (38) and (39) this source/sink term cancels out, since we take/put mass with the same lever arm as angular momentum is taken/put in (cf. the situation for $R = R_A$ in Mayer & Pringle 2006). Thus we get for the disc

$$\dot{M}_d \frac{\partial (R^2 \Omega_d)}{\partial R} = \frac{\partial G_d}{\partial R}, \quad (40)$$

and for the corona

$$\dot{M}_c \frac{\partial (R^2 \Omega_c)}{\partial R} = \frac{\partial G_c}{\partial R}, \quad (41)$$

where Ω_d and Ω_c are the respective rotation frequencies which we take to be Keplerian, i.e. $\Omega_d = \Omega_c = \sqrt{GM/R^3}$.

4.2 Conductive heat transport

In Sect. 2.3 we calculate a mass transfer rate owing to the imbalance of heating and cooling in the transition layer (eq. 26).

If the hot corona condenses into the disc ($\dot{m}_z < 0$), the residual heat is transferred to the corona at a rate $S_{\text{cond}} = -\dot{m}_z e_c$. If the disc evaporates into the hot corona ($\dot{m}_z > 0$), the corona is heated at a rate $S_{\text{cond}} = \dot{m}_z e_d$. Thus

$$S_{\text{cond}} = \begin{cases} -\dot{m}_z e_c & \text{if } \dot{m}_z < 0 \text{ (corona condenses),} \\ \dot{m}_z e_d & \text{if } \dot{m}_z > 0 \text{ (disc evaporates).} \end{cases} \quad (42)$$

e_d and e_c are the specific internal energies per unit mass in the disc and corona (cf. eqns. A1 and A2).

4.3 Energy equations

The energy equation for the disc is

$$\frac{\partial}{\partial t} (\Sigma_d e_d) + P_d \dot{H}_d = -\frac{1}{2\pi R} \frac{\partial}{\partial R} (\dot{M}_d e_d) - \frac{P_d}{2\pi R} \frac{\partial}{\partial R} \left(\frac{\dot{M}_d}{\rho_d} \right) + (Q_d^+ + Q_{\text{heat},d} - \Lambda_d^-) - S_{\text{cond}}, \quad (43)$$

where Σ_d , e_d , P_d and H_d are the surface density, specific internal energy per unit mass (A1), Pressure (2) and scale-height in the disc. Q_d^+ and Λ_d^- are the local heating and cooling rates (cf. eq. 6 and 3), $Q_{\text{heat},d}$ the heating by the impinging radiation of the corona (cf. eq. 15) and S_{cond} the heat source/sink term for conduction (42). The first two terms on the right hand side represent the radial advection of energy and 'pdV'-work, while the others represent local source/sink terms.

The energy equation for the corona is split into one for the electrons and one for the protons. We write for the protons

$$\frac{\partial}{\partial t} (\Sigma_c e_{p,c}) + P_{p,c} \dot{H}_c = -\frac{1}{2\pi R} \frac{\partial}{\partial R} (\dot{M}_c e_{p,c}) - \frac{P_{p,c}}{2\pi R} \frac{\partial}{\partial R} \left(\frac{\dot{M}_c}{\rho_c} \right) + (Q_{p,c}^+ - Q_{\text{ep}} - \Lambda_{\text{brems},p}) + S_{\text{cond}} \frac{e_{p,c}}{e_c}, \quad (44)$$

and

$$\frac{\partial}{\partial t} (\Sigma_c e_{e,c}) + P_{e,c} \dot{H}_c = -\frac{1}{2\pi R} \frac{\partial}{\partial R} (\dot{M}_c e_{e,c}) - \frac{P_{e,c}}{2\pi R} \frac{\partial}{\partial R} \left(\frac{\dot{M}_c}{\rho_c} \right) + (Q_{e,c}^+ + Q_{\text{ep}} - \Lambda_{\text{brems},e} - \Lambda_{e,c,C}^-) + S_{\text{cond}} \frac{e_{e,c}}{e_c}, \quad (45)$$

where Σ_c , $e_{p,c}/e_{e,c}$, $P_{p,c}/P_{e,c}$ and H_c are the surface density, specific internal energy per unit mass (A2), Pressure (9) and scale-height of the corona. The pressure and internal energy is split into the respective fraction for protons and electrons. $Q_{p,c}^+$ and $Q_{e,c}^+$ are the heating rates for protons and electrons, respectively (see eqns. 11, 12 and 13), Q_{ep} the electron-proton collision rate and $\Lambda_{\text{brems},p}$ and $\Lambda_{\text{brems},e}$ the electron-proton bremsstrahlung rate owing to the contributions

of protons and electrons, respectively. $\Lambda_{e,c,C}^-$ is the Compton cooling/heating term (eq. 14). The first two terms on the right hand side of eq. (44) and (45) represent the radial advection of energy and the 'pdV'-work, while the others are local source/sink terms.

Note that Q_{ep} is an interaction term and is treated as such in the energy equations. It conserves energy since the Coulomb collisions transfer energy from the protons to the electrons. The combined energy equation for the corona, the sum of eq. (44) and (45) does reflect this. The conductive energy transport conserves energy as well as is evident from the sum of all three energy equations. The same applies for the conductive mass exchange in the continuity equations.

5 NUMERICAL SETUP

Here we discuss the numerical scheme, the initial setup and the boundary conditions used in this paper. As we discussed above, the numerical results presented here are severely limited by the numerical resources required. We use a logarithmically equidistant grid with typically $N = 30$ points starting from $R = 3 R_S$ to $R = 3000 R_S$. All variables except the coronal and disc accretion rate \dot{M}_c and \dot{M}_d are defined on the grid point. The accretion rate then is defined in between the grid points as is evident from eq. (40) and (41).

We take initial values for our simulation from a stationary model where we neglect radial advection and conduction. The (initial) accretion rates in the corona and disc are $f_c \dot{M}$ and $(1 - f_c) \dot{M}$, respectively.

We integrate the system of time-dependent equations with a one-step Euler scheme and treat the advection terms in a first-order, upwind donor cell procedure. We have written our scheme so that we conserve mass and energy to machine accuracy.

At the inner boundary we impose a zero-torque condition ($G_d(R_{in}) = G_c(R_{in}) = 0$). This is equivalent to setting $\Sigma_c(R_{in}) = \Sigma_d(R_{in}) = 0$. All matter and energy flowing through this inner boundary is lost from the system. It is either added to the black hole or lost in a jet. No advection of energy and mass from within the inner radius is allowed.

At the outer boundary we set the accretion rate $\dot{M} = 0$ for both the disc and corona. Just inside the outer boundary at the last disc cell, we supply mass to the optically thick disc at a fixed rate $\dot{M}_0 = (1 - f_c) \dot{M}$. Energy corresponding to the internal energy of the last disc cell is put into the last disc cell at a rate $(1 - f_c) \dot{M} e_d$. No mass nor energy is supplied to the corona. Thus \dot{M}_0 is the only parameter characterising the system. The accretion flow then evolves self-consistently within the model and mass is transferred between the two phases accordingly.

As one of the computationally more intensive parts of the simulation is the calculation of the evaporation/condensation rate (26), we use tables for essential parts of the integral and use interpolations in the course of the simulations. This enables us to calculate the evaporation/condensation rate with sufficient accuracy without spending too much computational time on the calculation.

The computational time involved in the simulations is considerable. Since the geometries of the disc and corona are very dissimilar (the disc is geometrically thin while the corona is geometrically thick), the viscous timescales are vastly different. The viscous timescale is (e.g. Pringle 1981)

$$\tau_v = \frac{1}{\alpha \Omega_K (H/R)^2}, \quad (46)$$

which in units suitable for the presented models leads to a value of

$$\tau_v = 1.4 \cdot 10^{-3} \text{ s} \cdot \left(\frac{\alpha}{0.1} \right)^{-1} \left(\frac{M}{10 M_\odot} \right) \left(\frac{R}{R_S} \right)^{\frac{3}{2}} \left(\frac{H}{R} \right)^{-2}. \quad (47)$$

For the disc usually the ratio between scale-height and radial distance from the black hole $H/R \approx 10^{-2}$, while for the corona $H/R \approx 1$. Thus the ratio of the viscous timescale of the disc and corona at a given radius is about 10^4 . Thus it takes 10^4 times longer for the disc to reach a (possibly) viscous equilibrium than for the corona. The thermal and hydrostatic timescales, however are similar.

Numerically the viscous evolution allows for time steps smaller than (Bath & Pringle 1981)

$$\Delta t < \frac{1}{2} \frac{R \Delta R}{12 \alpha \Omega_K H^2}. \quad (48)$$

For $\alpha = 0.1$, $H \approx R$ and $\Delta R = \delta R$ with $\delta < 1$, it is evident, that the maximum allowed time step for the viscous evolution is close to or even below the dynamical timescale.

The dynamical timescale at the outer boundary at $R = 3000 R_S$ is about 230 s, i.e. we need to integrate about $2 \cdot 10^5$ times the dynamical timescale of the innermost orbit to reach the dynamical timescale and another 10^4 times to calculate for one viscous time at the outer boundary at $R = 3000 R_S$. We then arrive at about $2.3 \cdot 10^6$ s to be calculated in real time, using about $2 \cdot 10^9$ time steps.

Given the different timescales involved in this problem, an implicit solver would be ideally be suitable. We however chose to use an explicit solver since implicit solvers usually have problems with switching on/off processes (here mainly the mass transfer of eq. 26 which switches signs depending on the cooling and heating in the transition layer) given their large extrapolation capability. The disadvantage of the explicit solver then is the large number of time steps needed to evolve the disc.

In order to save computational time, we can make further approximations. Formally all five time-dependent equations constitute a coupled system for the time-dependent variables Σ_d , Σ_c , e_d , $e_{p,c}$ and $e_{e,c}$ (eqns. 38, 39, 43, 44 and 45). All the other variables at a given time can be calculated considering hydrostatic equilibria (eq. 1) and (8) and the respective expressions for the pressure (2) and (9) and energy (A1 and A2). This system of 5 equations can be reduced to a system of 3 equations (see eq. A1 and A3 – A4) but then it only can be solved numerically. However with a few simplifications a (computationally expensive) numerical solution can be avoided. It is evident that since generally $H_d \ll H_c$, H_d can safely be neglected in (8). As we only consider only a disc with very low accretion rates, we also can neglect radiation for the disc pressure and internal energy (second term on the right hand sides of eqns. 2 and A1). By applying these approximations, we can analytically solve the five equations and hence avoid unnecessary numerical iterations. The same applies to the terms involving \dot{H} in both the coronal (eqns. 44 and 45) and disc (43) energy equation. A change dH can be expressed in terms of the surface density and internal energy of the disc and corona (see eqns. A5 and A6). In the course of this paper, we choose to neglect this term in order to save computational time. Physically this is justified since the corona and disc only influence each other through this term if the pressure in the disc and corona are close to each other or the scale-height of the disc and corona are similar (cf. eqns. A5 and A6). Then however the disc or corona ceases to exist and other measures need to be taken (cf. Sect. 2.4). In all cases other than that the coupling involving the \dot{H} terms is negligible.

5.1 Disc develops a hole

Our recipe for the truncated part of the disc are as follows. If the surface density of the disc falls below 80 per cent of the surface density of the corona, the disc does not exist any more. The corresponding cell however is allowed to advect mass and energy from the neighbouring still active disc cell. The disc is “reborn”, if the “dead” disc surface density has refilled up to 90 per cent of the coronal surface density. “Dead” disc cells do not have thermal conduction, produce no torque, are neither heated by the corona nor by viscous dissipation. The corona in this parts of the flow is cooled by soft photons from the outer and inner (as long as it exists) disc parts (cf. Sect. 2.4). The innermost cell of the outer disc is defined as the cell where most of the mass is evaporated in the corona. The outermost cell of the inner remnant disc still loses mass to the next “dead cell” for angular momentum conservation. If the surface density, i.e. mass, of the disc in this cell is sufficiently high, then the disc is reactivated again. As the surface area of the disc annuli increases proportionally to R^2 , the outwards advected mass hardly ever manages to reactivate a disc cell.

5.2 Corona fully condenses into disc

This case does not occur in the model presented in this paper. If the corona did fully condense into the disc, then the corresponding torques and accretion rates in this parts of the corona decrease towards zero. If the scale-height of the corona shrinks below some limit (Physically we should take the point when the optical depth with respect to absorption becomes larger than unity), this part of the flow then is in a disc only state. Mass and energy influx from either side into the corona is still allowed. The corona starts to exist again if the optical absorption depth of the corona has shrunk below a certain threshold.

6 RESULTS

In the calculation we describe here, we consider an accretion disc model for a $10 M_\odot$ black hole accreting at $10^{-3} \dot{M}_{\text{Edd}}$. We describe the time-evolution below.

In Fig. 3 we show a schematic view of a typical sandwich disc in the initial stage of the time-evolution. We show relevant actual physical quantities 0.1, 20, 50 and 100 kiloseconds after the start of the simulation in Figs. 4-7.

We start with a stationary disc and corona extending over the total computational domain. To compute the initial disc and corona structure we neglect radial advection, and we take the fraction of accretion occurring in the corona as $f_c = 0.1$.

Initially (Fig. 4) in the outer regions the disc begins to evaporate into the corona, whereas in the inner regions the corona begins to condense into the disc (see Panel 1 in Fig. 3). Since the disc loses a lot of matter in the outer parts by evaporation into the corona, the corona temporarily starts to flow outwards (Fig. 4d). Most of the matter is in the disc, and the corona is two-temperature inside a radius of $R \approx 100 R_S$.

Although the corona close to the black hole has got a very small surface density in the initial model, as the outer disc however evaporates mass into the corona, this matter is then transported inwards through the corona. Further in, the coronal accretion rate decreases as part of the coronal matter condenses into the disc and fills up the corona to surface densities of about $0.3 \dots 1 \text{ g cm}^{-2}$. This process happens very quickly, i.e. on the viscous timescale

of the corona. The increase in coronal mass in the inner regions leads to an increase in the coronal luminosity. The inner corona itself condenses into the disc and increases the disc surface density (compare Fig. 4b and 5b). Since most of the matter condenses very close to the actual transition radius between the evaporating disc and recondensing corona (which starts at around $R \approx 300 R_S$ and increases eventually to around $R \approx 1000 R_S$), it takes about a viscous timescale of the disc at that radius to increase the surface density of the inner disc. This timescale is 10^4 times longer compared to the viscous timescale of the corona.

At the transition radius (where the flow changes from an evaporating disc to and recondensing corona), the disc starts to flow outwards (see Panel 1 in Fig. 3 and Fig. 5d). The accretion flow in the disc is then divided into three zones. In the inner zone the disc is moving inwards, in the intermediate zone it is moving outwards, and all the accretion is carried by the corona. In the outer zone the disc is moving inwards. At the boundary of the intermediate and the outer zone, despite the fact that the disc flow is towards this radius, the surface density of the disc declines rapidly. This comes about because most of the mass flowing into this region from both sides is quickly evaporated into the corona. An empty ring, or gap, develops in the disc at this point. This gap consists of coronal gas only and is Compton cooled by soft photons from both the outer and inner disc remnants.

Once this gap has formed (Fig. 6), the inner disc is accreted and the gap widens. A decline in the disc scale-height is already visible in Fig. 5c, but the truncation of the disc is fully evident in Fig. 6. The inner disc disperses. This state is shown schematically in Panel 2 of Fig. 3.

Most of the inner disc gets accreted while a small part flows outwards (see Fig. 6d). The luminosity of the disc declines. Eventually we are left with an accretion flow where the inner part consists of a corona only and the mass supply for this corona is produced by the outer remnant disc (cf. Panel 3 of Fig. 3 and Fig. 7).

We show the luminosity evolution of the corona and disc in Fig. 8. Initially, the luminosity of the corona increases very quickly (caused as we described above by a filling of the inner parts of the corona on the short viscous timescale of the corona at the transition from the two- to a one-temperature plasma), but cannot exceed the disc luminosity as long as a disc exists (see Sect. 3). On the much longer, viscous timescale of the disc the disc luminosity increases (causes by a steady increase of surface density of the inner disc), before the luminosity drops with the development of the gap. Once the inner disc is completely accreted, the dominant part of the radiation comes from the hot corona. The disc becomes steady-state at this point, and no significant further evolution occurs.

7 DISCUSSION

The results of these computations indicate that a disc around a $10 M_\odot$ black hole, accreting at $\dot{M} = 0.001 M_{\text{Edd}}$ relaxes to a state in which the outer disc is a standard accretion disc with a small corona, but the inner regions ($R \lesssim 1000 R_S$) consist of only hot coronal gas which has evaporated from the disc.

7.1 Thermal conduction and the transition from condensation to evaporation

These calculations basically agree with the results of Różańska & Czerny (2000b) who concluded that for a stationary disc there would be net condensation of the corona in the

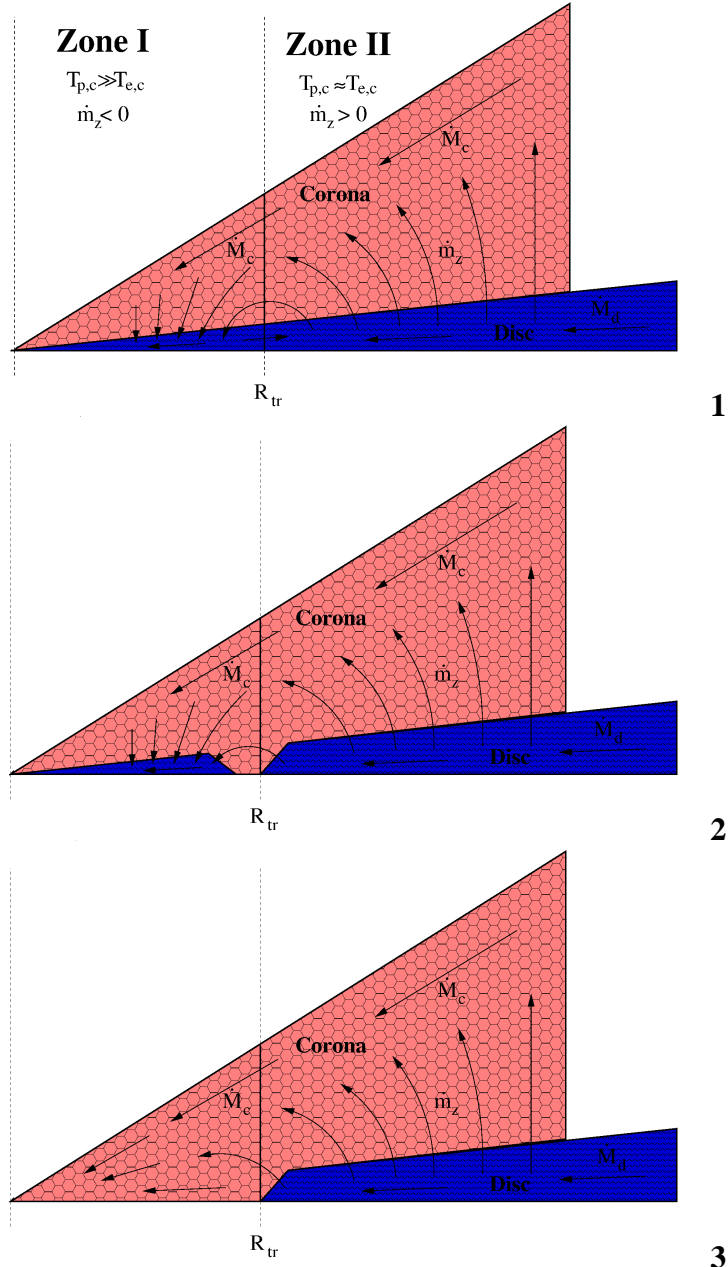


Figure 3. Schematic view of a typical sandwich disc in the course of the time-evolution. We only show one side of the sandwich. The sandwich is symmetric with respect to the horizontal axis. The arrows indicate the mass flow within the corona (light red) and within the disc (blue) as well as the conductive mass flow between the two phases. The flow radially comprises of three zones: In Zone II (one-temperature corona) the disc evaporates leading to the formation of a corona. The evaporated mass flows inwards within the corona. In Zone I (two-temperature corona) the corona condenses into the disc. Both the disc and the corona accrete in this zone. At about the transition radius R_{tr} disc flows outwards (Panel 1). After some time, the disc is truncated and the hole is filled with coronal gas (Panel 2). The inner disc quickly gets accreted and the system is left with the situation as shown in Panel 3.

inner disc and net evaporation further out. This comes about for the following reasons.

The calculation of the evaporation/condensation rate (eq. 26) shows that the sign of the term $(q_{TL}^+ - q_{TL}^-)$ determines condensation and evaporation, while the κ_{cond} term given its strong temperature dependence determines the magnitude of the condensation/evaporation. This strong temperature dependence also ensures that for the heating and cooling mechanisms considered in this paper the mass transfer rate mainly depends on the upper boundary of the integration, i.e. the coronal values for the temperature.

To get an idea what causes the evaporation/condensation in the two zones shown in Fig. 3 we assume that the only heating is the αP_c heating (22) and Compton cooling (23) and bremsstrahlung are the only cooling mechanisms.

Within the corona the system is usually in thermodynamical equilibrium or quickly relaxes back to equilibrium – faster closer to the black hole than further out.

In the two-temperature plasma (zone I) Compton cooling dominates. If we calculate the difference between volume heating

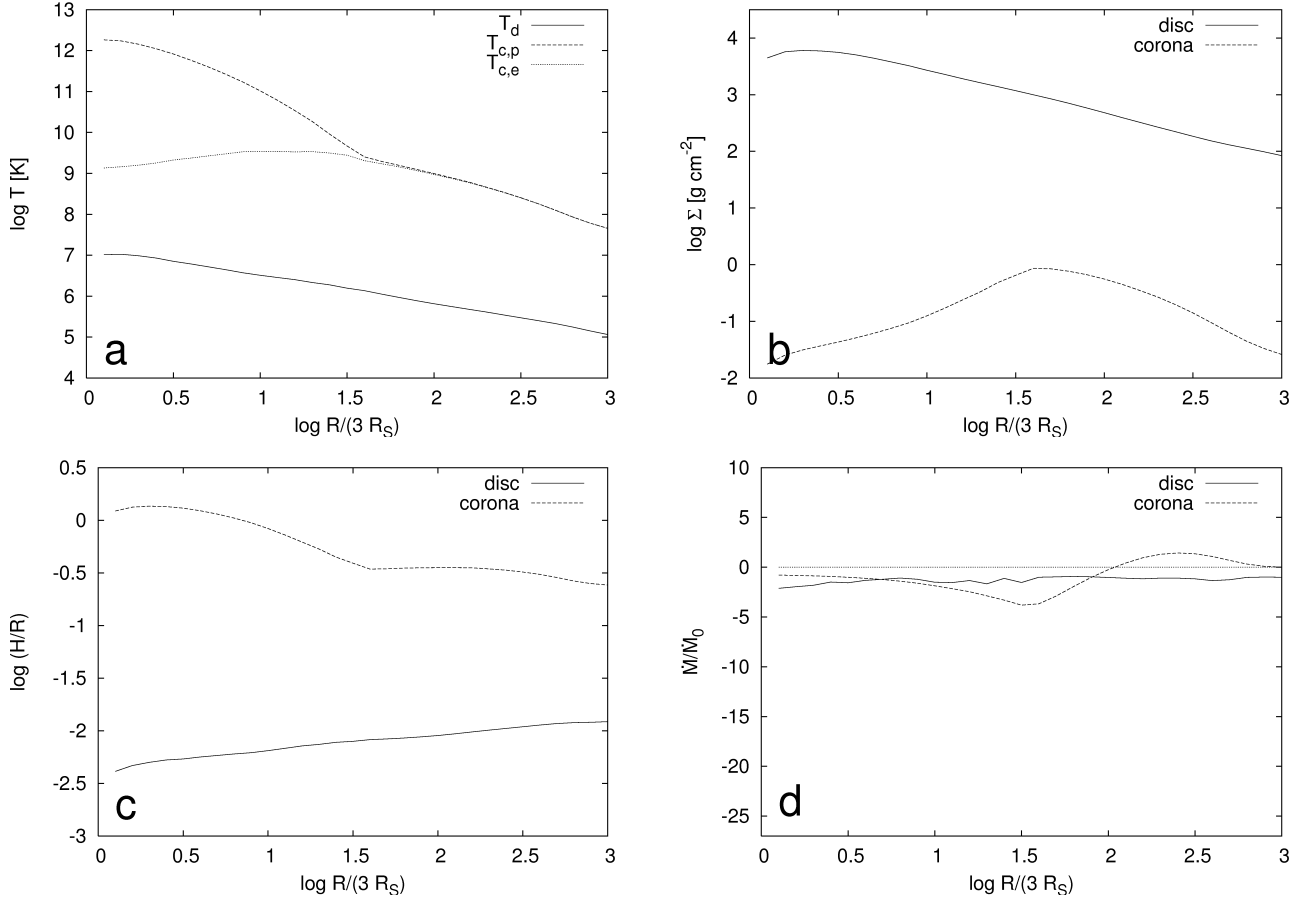


Figure 4. Some physical quantities in the time-evolution of the accretion flow 100 s after the start of the simulation: Panel a shows the electron and proton temperature in the corona and the temperature of the disc, Panel b,c, and d show the surface density, the ratio (H/R) and the accretion rate for disc and corona, respectively. Note that we normalized the accretion rate to the rate we feed the disc in the outermost grid cell. The disc is evaporating in its outer parts very strongly and leads to an outflowing corona beyond a critical radius (see Panel d).

and cooling, we get

$$q_c^+ - q_{c,C}^- = P_c \left(\alpha_c \Omega_c - 8 \kappa_{es} \mu m_p \frac{T_e}{T_e + T_p} \frac{\sigma T_{\text{eff},d}^4}{m_e c^2} \right), \quad (49)$$

where we have neglected Compton heating and the relativistic generalisation in (23). Within the corona, this term is about zero (assuming thermal equilibrium). To get the evaporation/condensation rate, we need to integrate the difference over the range of temperatures from the disc to the coronal values. If the corona is a two-temperature plasma, then the fraction $T_e/(T_e + T_p)$ is small, but the closer we get to the one-temperature plasma within the transition layer, the bigger it becomes. Then the difference (49) becomes increasingly negative. The corona condenses onto the disc.

In zone II we have got a one-temperature plasma and Bremsstrahlung dominates the cooling. We need to calculate (For simplicity we use the classical Bremsstrahlung result, i.e. $q_{c,\text{brems}} \propto \rho^2 T^{1/2}$)

$$q_c^+ - q_{c,\text{brems}}^- = P_c \left(\alpha_c \Omega_c - C \frac{P_c}{T^{3/2}} \right), \quad (50)$$

where C is an arbitrary constant of proportionality. While the difference is zero in the corona, the further down we integrate towards the disc temperature, the smaller gets T and the larger the second term in the difference. Cooling dominates heating in the transition

layer and thus the corona condenses into the disc. This is in contrast with our results presented in Section 6. The outer parts of the disc evaporate because the outward advection in the initial phases of the disc evolution lead to an imbalance between heating and cooling. Heating dominates there and hence the disc evaporates.

7.2 Physical processes neglected in this model

We now discuss some of the additional physical processes which we have neglected here, but which will need to be taken into account if the model is to be developed further.

7.2.1 Other cooling mechanisms

Further out other cooling mechanisms than Compton cooling and bremsstrahlung will be more efficient and eventually lead to a condensation of the corona. We neglect atomic cooling and only allow for bremsstrahlung and Compton cooling for both the corona and the transition layer. The temperature dependence of bremsstrahlung and Compton cooling ensures that the evaporation/condensation rate (cf. eq. 26) only depends on the upper limits of the integral involved. If we needed to include cooling processes other than bremsstrahlung (i.e. atomic cooling etc.), then the calculation of the evaporation/condensation rate would be much more difficult. In

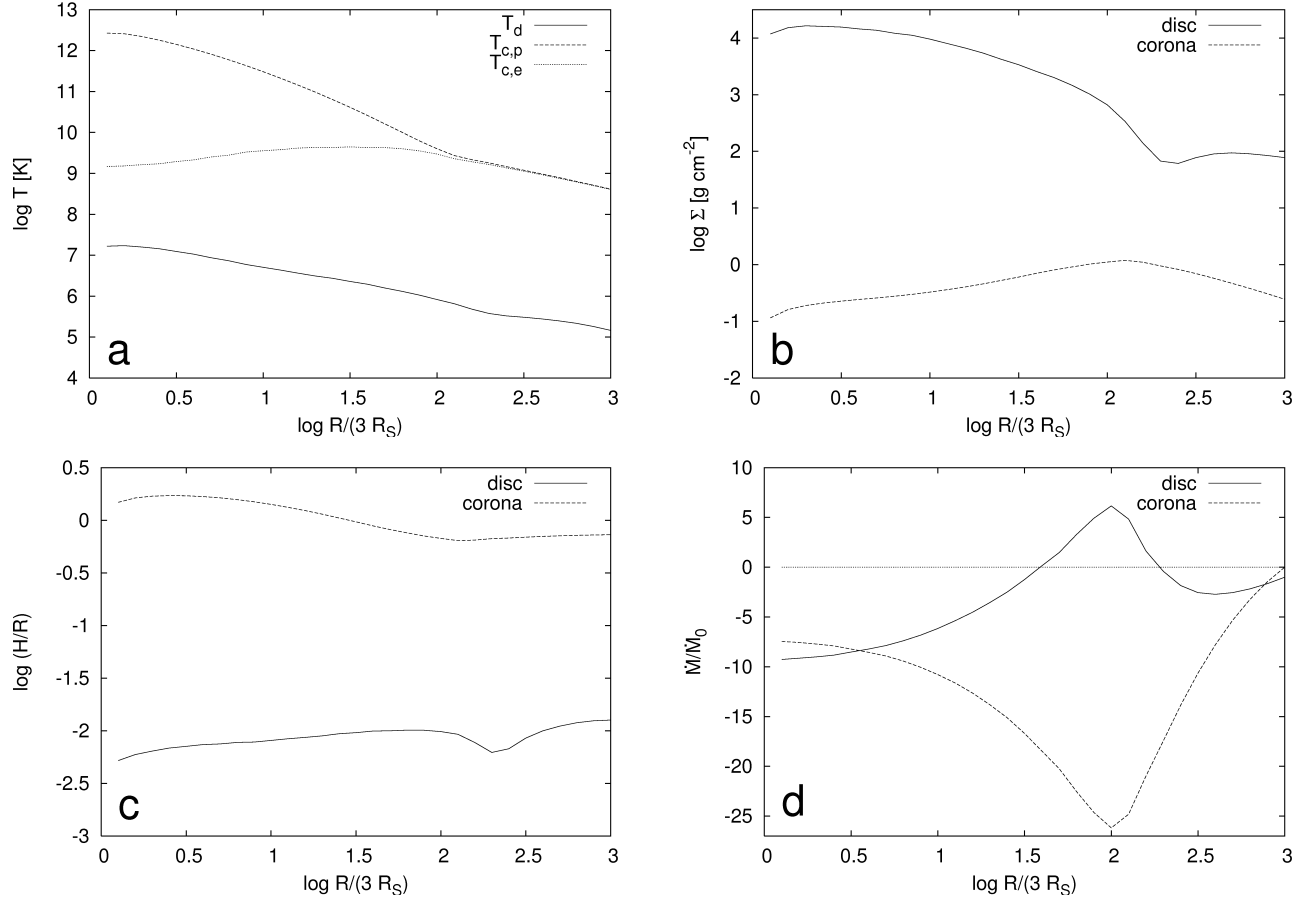


Figure 5. The accretion flow 20 ks after the start: The corona production is at its maximum and so is the accretion rate in the corona. Most of the corona is produced at the transition from the two- to one-temperature plasma. As a result the disc flows outwards in some parts. Note that the ratio H/R for the disc starts to decrease. The labelling is the same as in Fig. 4.

the transition layer the gas then can have a significant absorption optical depth which in turn leads to photoionisation processes and significant radiation pressure. Photoionisation and radiation pressure also influence the corona if it starts to collapse and may lead to an outflow (See Sect. 7.2.2). The increase in cooling may also be responsible for changing the sign of \dot{m}_z from evaporation to condensation in the outer parts of the disc and thus will stop the transition radius to move outwards.

With the widening of the inner gap a lack of soft photons develops and the electron temperature reaches temperatures in excess of 10^{10} K. This invalidates our use of non-relativistic Bremsstrahlung rates. However given the other underlying approximations in the model, the missing factors of a few should not influence the results too much. In a more realistic model, pair production will set in (e.g. Svensson 1982) and help to cool the corona. Pair production increases the electron scattering optical depth and thus also leads to a rise in the Compton cooling rate. In fact, many, if not all observations of AGN hint at the existence of a population of hot electrons in a very narrow range of electron temperatures (about 100 keV, which corresponds to 10^9 K for NGC 4151, see Beckmann et al. 2005). These authors deduce an optical depth for the corona of $\tau \approx 1.3$. This is much higher than the values encountered in the model presented in this paper.

The study of these cases is very important but requires further work.

7.2.2 Wind/Outflow

We have neglected the possibility of a wind/outflow throughout these calculations. Physically given the large ratio of H/R for the corona, the corona is only marginally bound within the gravitational potential (Blandford & Begelman 1999). Thus it may well be that mass, energy and angular momentum is carried away in an outflow, jet or wind. This might then eventually lead to a reduction of H/R until a stable state is found. This would then be an additional cooling mechanism for the corona. Observations of low-luminosity AGN and X-Ray binaries in their low/hard state indicate that they are dominated by large-scale outflows (Fender et al. 2004). These outflows can be driven magnetically (e.g. Mayer & Pringle 2006) or by radiation pressure as well (cf. Sect. 7.2.1).

7.2.3 Corona production

Another important question to be answered is the production of the corona. Our model presented in this paper shows that once we start with a tiny corona and consider thermal conduction, the corona is produced mainly from the outer optically thick disc. How the corona came into existence in the first place is not clear. As described in Sect. 2.4, we have run simulations for a one-phase black hole accretion disc but allowing for the transition to an optically thin flow. The simulations are similar to the ones reported in Mayer & Pringle (2006), except that we now use a prescription

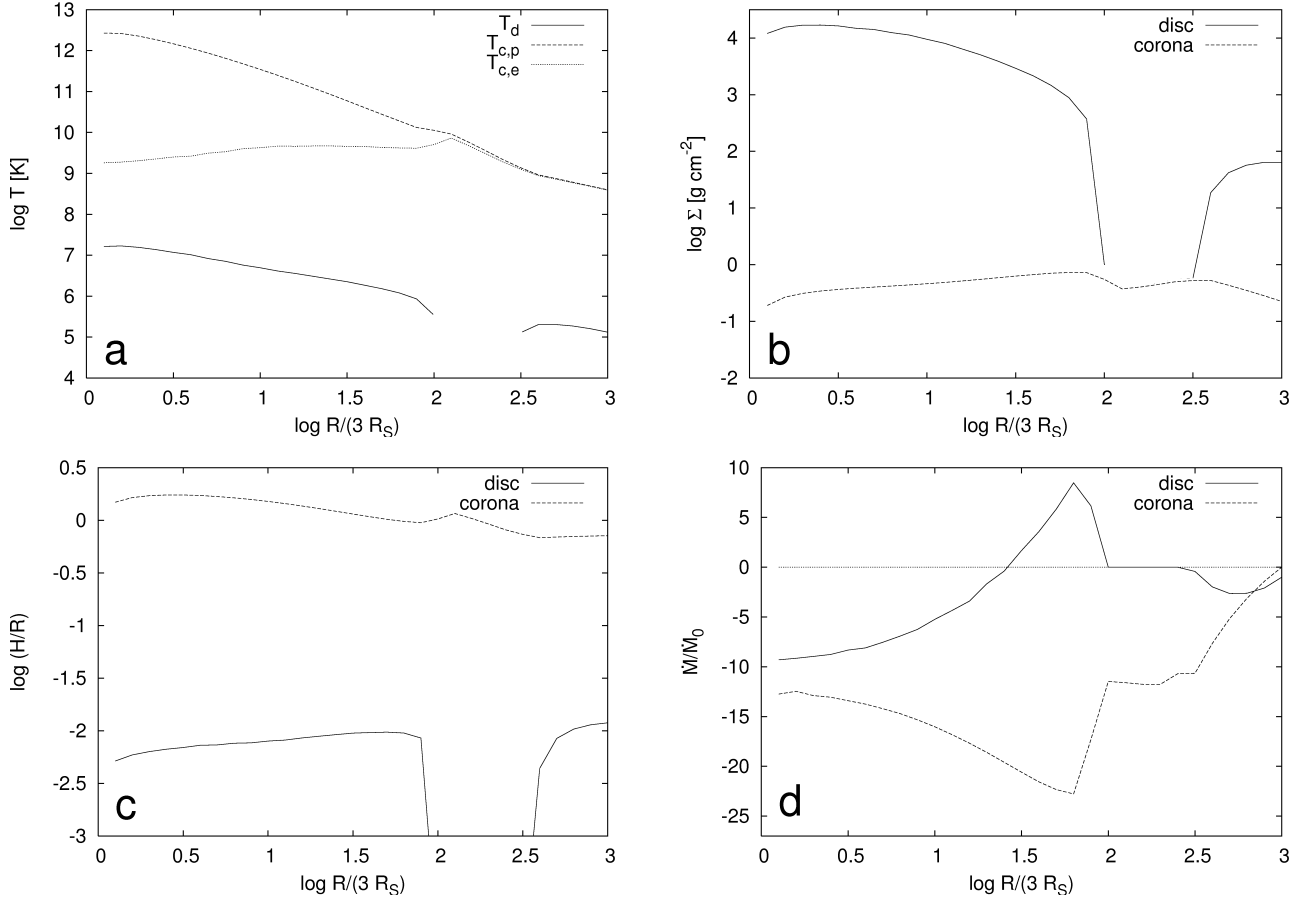


Figure 6. The accretion flow 50 ks after the start: The disc develops a gap and the accretion flow in the disc is truncated. The inner disc disperses, i.e. parts flow outwards, while most of the matter is accreted. The outer disc evaporates and produces the corona. The coronal accretion flow in the gap is stationary, i.e. the accretion rate is radially constant (see Panel d) given its much smaller viscous timescale. The labelling is the same as in Fig. 4.

by Artemova et al. (1996) for the optically thick-thin transition. As reported before, we still find limit cycles for the same range of accretion rates. During the high- \dot{M} phase, where the inner accretion disc is depleted, this part of the accretion flow becomes optically thin and the temperature rises to about 10^9 K close to the black hole. This might be a promising mechanism to produce a corona and a possible explanation for the so-called very high (VH) or steep power law (SPL) state in X-Ray binaries (Remillard & McClintock 2006). This optically thin coronal part (being geometrically thick) then can flow out-/inwards on top of the accretion disc.

7.2.4 Extra shear

In the course of this paper, we neglect non-Keplerian rotation for the corona. We here discuss some possible effects of the inclusion of non-Keplerian rotation into the model. These could play an important role in determining energy dissipation and the redistribution of angular momentum (i.e. accretion) in the disc and the corona. It will be important to investigate the outcome of including these effects in future computations.

Since the corona is geometrically thick, radial pressure gradients lead to a deviation from pure Keplerian rotation. Corona and disc thus rotate at different speeds. At their boundary (the transition layer) torques arise which lead to angular momentum exchange between the two phases. The work done by these torques leads to

an additional heating of the corona, in particular the ions. Further angular momentum exchange arises from the mass transfer due to thermal conduction as then both layers rotate on different speeds. We give here a rough calculation of the torques and dissipation rates which might arise from these processes and the effect of the extra torque on the accretion flow.

The rotation frequency $\Omega_c \neq \Omega_K = \sqrt{GM/R^3}$ in the presence of a radial pressure gradient is given by

$$\Omega_c = \sqrt{\Omega_K^2 + \frac{1}{\rho_c R} \frac{\partial P_c}{\partial R}}, \quad (51)$$

where ρ_c is the coronal density, P_c the pressure and R the radial distance from the black hole. We approximate the pressure gradient by $\partial P_c / \partial R = P / R \chi_P$ with $\chi_P = \partial \log P_c / \partial \log R$. Since $P_c \approx \rho_c c_{s,c}^2$ and $c_{s,c} \approx \Omega_c H_c$, where $c_{s,c}$ is the sound speed and H_c is the scale-height of the corona, we get

$$\Omega_c = \frac{\Omega_K}{\sqrt{1 - (H_c/R)^2} \chi_P}. \quad (52)$$

If $\Delta\Omega = \Omega_K - \Omega_c$, then for small $H_c/R < 1$ we can write

$$\frac{\Delta\Omega}{\Omega_K} = -\frac{1}{2} \left(\frac{H_c}{R} \right)^2 \chi_P. \quad (53)$$

Thus coronal and disc flow rotate at different speeds. The differential

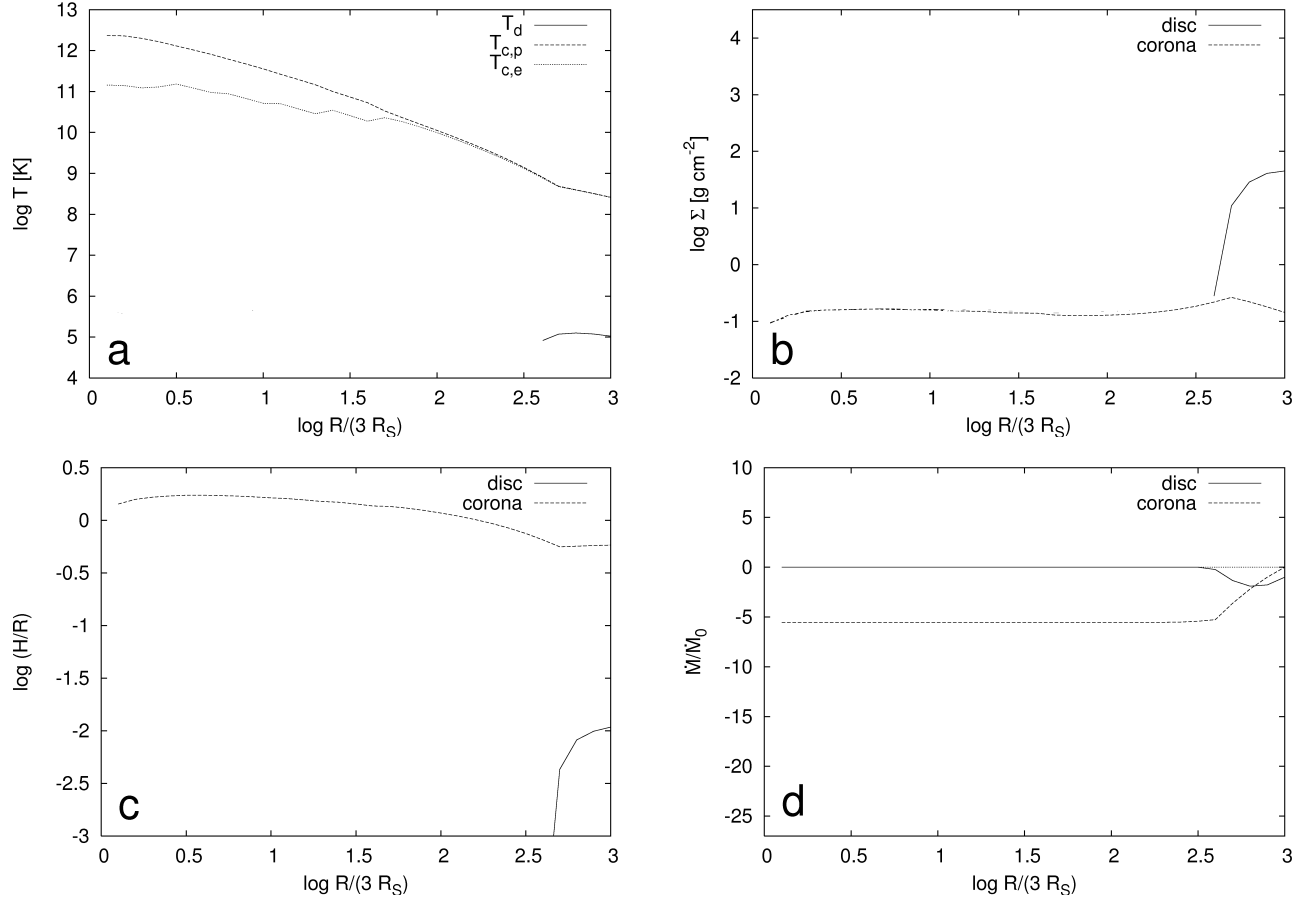


Figure 7. The accretion flow 100 ks after the start: The inner disc completely dissolved by accretion and the inner parts of the flow consist only of a hot corona. This part of the corona is stationary. Further out there still is a remnant accretion disc producing the corona. The labelling is the same as in Fig. 4.

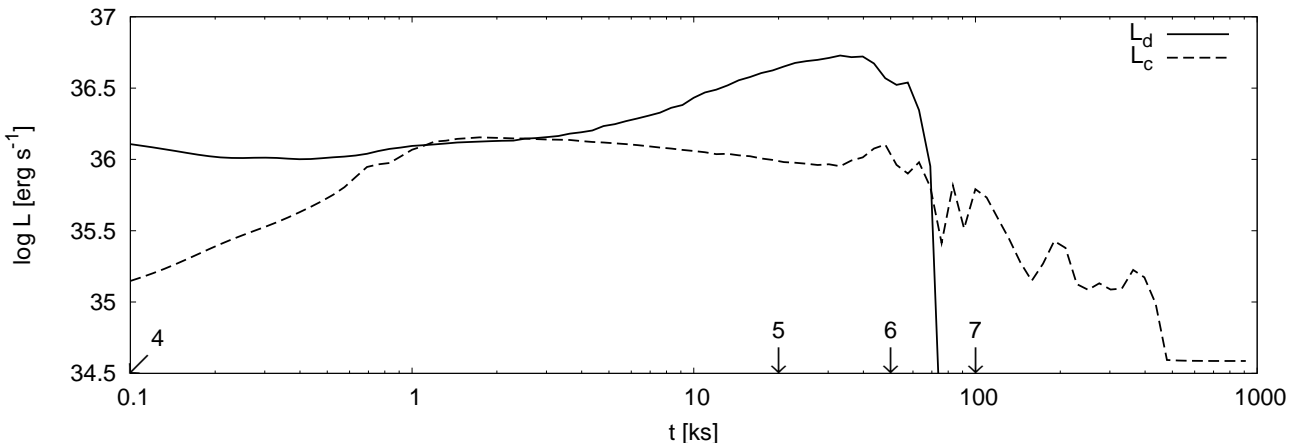


Figure 8. Luminosity of the disc L_d and corona L_c . Initially the coronal luminosity increases quickly for 1 ks. Then the corona condenses into the inner disc leading to an increase in the disc luminosity (cf. Fig. 4 and 5). Starting at 40 ks, the disc luminosity declines as the gap widens. After about 70 ks the disc luminosity declines rapidly (The inner disc dissolves, cf. Fig. 6 and 7) and the corona dominates the luminosity. The small-amplitude variations in the luminosity arise from the coarse resolution and numerical fluctuations. The numbers annotated to the arrows on the time axis correspond to the figure number representing the respective state of the system. Note that we use a logarithmic scale for the time to differentiate the highlight the various timescales.

rotation leads to a free energy per unit surface area of about

$$\Delta E_c = \frac{1}{2} \frac{\Sigma_d \Sigma_c}{\Sigma_d + \Sigma_c} (\Delta \Omega R)^2. \quad (54)$$

We note that usually $\Sigma_d \gg \Sigma_c$ and thus $\Delta E_c \approx \frac{1}{2} \Sigma_c (\Delta \Omega R)^2$. This energy is released on a multiple of the local dynamical timescale, i.e. we set

$$\Delta t_{E_c} = f_{E_c} \Omega_c^{-1}, \quad (55)$$

where $f_{E_c} \geq 1$ is a parameter and Ω_c^{-1} the dynamical timescale. The release of the free energy (54) leads to an additional heating of the corona at a rate

$$Q_{c,diff} \equiv \frac{\Delta E}{\Delta t} = \frac{1}{2} \frac{\Sigma_d \Sigma_c}{\Sigma_d + \Sigma_c} (\Delta \Omega R)^2 \Omega_c f_{E_c}^{-1}. \quad (56)$$

If we put (53) into the last equation, then we get

$$Q_{c,diff} = \frac{1}{8} \frac{\Sigma_d \Sigma_c}{\Sigma_d + \Sigma_c} (\Omega_K R)^2 \left(\frac{H_c}{R} \right)^4 \chi_P^2 \Omega_c f_{E_c}^{-1}. \quad (57)$$

The heating timescale for this process is

$$\tau_{diff,c} \equiv \frac{\Sigma_c c_{s,c}^2}{Q_{c,diff}} = 8 \frac{\Sigma_d + \Sigma_c}{\Sigma_d} \left(\frac{R}{H_c} \right)^2 \left(\frac{\Omega_c}{\Omega_K} \right)^2 \chi_P^{-2} f_{E_c} \Omega_c^{-1}. \quad (58)$$

Thus the heating timescale is longer than the thermal timescale τ_c of the corona ($\tau_c \approx (\alpha_c \Omega_c)^{-1}$) for

$$f_{E_c} > \frac{1}{8 \alpha_c} \left(\frac{\Omega_K}{\Omega_c} \right)^2 \left(\frac{H_c}{R} \right)^2 \chi_P^2. \quad (59)$$

The differential rotation leads to a torque which tries to speed up the corona and slow down the disc, i.e. the torque is

$$G_{diff} \approx Q_{c,diff} / \Omega_c = \frac{1}{8} \frac{\Sigma_d \Sigma_c}{\Sigma_d + \Sigma_c} (\Omega_K R)^2 \left(\frac{H_c}{R} \right)^4 \chi_P^{-2} f_{E_c}^{-1}. \quad (60)$$

If only the torques given in eqns. (10) and (5) would be at work in the corona and disc, respectively, then in a stationary Keplerian disc (neglecting mass exchange due to thermal conduction) matter flows at a speed

$$u_{R,visc} = \frac{1}{2} \alpha c_s \left(\frac{H}{R} \right) \chi_\Omega \approx \frac{1}{2} \Omega R \left(\frac{H}{R} \right)^2 \chi_\Omega. \quad (61)$$

As long as Ω decreases with increasing radial distance, i.e. $\chi_\Omega = (\partial \log \Omega) / (\partial \log R) \approx -3/2 < 0$, then matter always flows inwards as expected. If we include the effects of the extra torque (60), then the contribution to the speed of matter is

$$u_{R,diff} = \frac{G_{diff}}{\Sigma R \Omega (2 + \chi_\Omega)}. \quad (62)$$

For a near Keplerian rotating flow we approximate $\chi_\Omega = -3/2$ and put in eq. (60) to get

$$u_{R,diff,c} = + \frac{1}{8} \frac{\Sigma_d}{\Sigma_d + \Sigma_c} \left(\frac{\Omega_K}{\Omega_c} \right)^2 \left(\frac{H_c}{R} \right)^4 \chi_P^2 f_{E_c}^{-1} \Omega_c R \quad (63)$$

and

$$u_{R,diff,d} = - \frac{1}{8} \frac{\Sigma_c}{\Sigma_d + \Sigma_c} \left(\frac{H_c}{R} \right)^4 \chi_P^2 f_{E_c}^{-1} \Omega_K R \quad (64)$$

for corona and disc, respectively. The relative contribution to the inflow caused by the viscous torques are

$$\frac{u_{R,diff,c}}{u_{R,visc,c}} = - \frac{1}{4 \alpha_c} \frac{\Sigma_d}{\Sigma_d + \Sigma_c} \left(\frac{\Omega_K}{\Omega_c} \right) \left(\frac{H_c}{R} \right)^2 \chi_P^2 f_{E_c}^{-1} \quad (65)$$

and

$$\frac{u_{R,diff,d}}{u_{R,visc,d}} = \frac{1}{4 \alpha_d} \frac{\Sigma_c}{\Sigma_d + \Sigma_c} \left(\frac{\Omega_K}{\Omega_c} \right) \left(\frac{H_c}{R} \right)^2 \left(\frac{H_c}{H_d} \right)^2 \chi_P^2 f_{E_c}^{-1}. \quad (66)$$

Thus for

$$f_{E_c} < \frac{1}{4 \alpha_c} \frac{\Sigma_d}{\Sigma_d + \Sigma_c} \left(\frac{\Omega_K}{\Omega_c} \right) \left(\frac{H_c}{R} \right)^2 \chi_P^2 \quad (67)$$

the corona starts to flow outwards and for

$$f_{E_c} < \frac{1}{4 \alpha_d} \frac{\Sigma_c}{\Sigma_d + \Sigma_c} \left(\frac{\Omega_K}{\Omega_c} \right) \left(\frac{H_c}{R} \right)^2 \left(\frac{H_c}{H_d} \right)^2 \chi_P^2 \quad (68)$$

the inflow speed of the disc is dominated by the extra torque.

For a typical disc and corona, we have $\chi_P \approx -1$, $H_c/R \approx 1$, $H_d/R \approx 10^{-2}$, $\Omega_c \approx \Omega_K/\sqrt{2}$ and $\Sigma_d \gg \Sigma_c$, then we have

- an outflowing corona for $f_{E_c} < 1/(4\alpha_c \sqrt{2})$
- and an inflowing disc dominated by the extra torque for $f_{E_c} < 10^4/(4\alpha_d \sqrt{2})$.
- Since we physically cannot resolve timescales smaller than the dynamical timescale, i.e. $f_{E_c} \geq 1$, α_c has to be smaller than $\alpha_c < 1/(4\sqrt{2}) \approx 0.18$ for both effects to work.

If we include the effects of thermal conduction, then the limit on f_{E_c} for the outflow of the corona decreases(increases) if the disc evaporates(corona condenses), since then the mass exchange transfers angular momentum as well. If the disc evaporates ($\dot{m}_z > 0$), the corona yields angular momentum at a rate of $\dot{m}_z R^2 \Delta \Omega$.

The extra torque can be produced by the poloidal component of the magnetic field, B_z , in the disc which slightly overextends into the corona. The smaller speed transforms the poloidal field into an azimuthal field. It creates an twist leading to a azimuthal field of the order of

$$B_\phi = -B_z \frac{\Delta \Omega}{\Omega_c} \quad (69)$$

after one orbit. Thus the torque produce by this process can be expressed as

$$T_{mag} = R \left(\frac{B_\phi B_z}{4\pi} \right) = R \frac{B_z^2}{4\pi} \frac{\Delta \Omega}{\Omega_c}. \quad (70)$$

We furthermore can assume that the poloidal magnetic field strength B_z is essentially equal to the intrinsic disc magnetic field B_{disc} . Thus we slightly underestimate B_{disc} . If we further use $B_{disc}^2 = 4\pi \alpha_d P_d$ (Shakura & Sunyaev 1973), then we can write for the torque in (70)

$$T_{mag} = R \frac{\Delta \Omega}{\Omega_c} \alpha_d P_d. \quad (71)$$

For $\Omega_c = \Omega_K/\sqrt{2}$ we get with eq. (53)

$$T_{mag} = -\sqrt{2} \left(\frac{H_c}{R} \right)^2 \alpha_d P_d \chi_P. \quad (72)$$

Finally we can use $P_d \approx \rho_d c_{s,d}^2 \approx \Sigma_d \Omega_K^2 H_d$ and arrive at

$$T_{mag} = -\alpha_d \sqrt{2} \left(\frac{H_d}{R} \right) \left(\frac{H_c}{R} \right)^2 \Sigma_d (\Omega_K R)^2 \chi_P. \quad (73)$$

The comparison of (72) and (60) allows to estimate f_{E_c} . We get

$$f_{E_c} = -\frac{1}{8 \alpha_d \sqrt{2}} \frac{\Sigma_c}{\Sigma_d + \Sigma_c} \left(\frac{H_c}{R} \right)^2 \chi_P^{-3} \left(\frac{H_d}{R} \right)^{-1} \quad (74)$$

For typical values for the corona ($\chi_P = -1$, $H_c \approx R$) and typical

values for the disc ($\Sigma_d \approx 10^{2...4} \Sigma_c$ and $H_d/R \approx 10^{-2}$) we get $f_{E_c} \approx (10^{-2} \dots 1)/(8\sqrt{2}\alpha_d)$. For $\alpha_d = 0.1$ this leads to $f_{E_c} \approx 10^{-2} \dots 1$. Since we underestimate B_{disc} , another factor larger than unity applies to the result in (74). Hence our estimate of f_{E_c} given the physical picture of the magnetic torque discussed above is compatible with an outflowing corona. It however constrains f_{E_c} to be not significantly larger than unity.

Note that the inclusion of thermal conduction introduces a non-constant accretion rate $\dot{M}_c(R)$ and $\dot{M}_d(R)$ for the corona and disc, respectively, even for the stationary case. Then extra factors enter the estimations presented above.

The physical process presented here might be responsible for driving a corona produced close to the black hole further outwards where it can be influence the spectrum and may condense into the disc (cf. Sect. 7.2.3).

8 CONCLUSIONS

We present time-dependent simulations for a two-phase accretion flow around a black hole. We start with a flow which initially consists of a cool and geometrically thin but optically thick accretion disc, sandwiched by a hot and geometrically thick but optically thin corona. We show that as the disc evolves, the disc-corona sandwich vanishes inside a certain radius. A gap in the disc develops and the inner disc is fully accreted. In the final state, we are left with a coronal hot inner flow and a disc-corona sandwich further out.

The general behaviour of the disc as described in this paper is not completely unexpected, since there is mounting evidence that the accretion flow around black holes at low accretion rates is truncated inside some radius (see Sect. 3). While we assume a stellar mass black hole of 10 solar masses, the result is likely also to apply to higher black hole masses, i.e. AGN. The result is in support of the unified scenario of Esin et al. (1997), where the optically thick disc is truncated below a certain radius for low accretion rates and only reaches the last stable orbit for higher accretion rates close to the Eddington limit.

For our model, we tried to keep the number of assumptions as small and the physics as simple as possible. But clearly there are still areas for improvement which we discuss in Section 7 and plan to include in the future work. The model presented here nevertheless gives an indication that the standard disc at low accretion rates cannot exist close to the black hole. The physical reasons for this are discussed in Section 7.1.

ACKNOWLEDGEMENTS

We gratefully acknowledge the use of a fast PC acquired for JEP by Emmanuel College, Cambridge. MM acknowledges support from PPARC. MM also thanks Massimo Cappi, Mauro Dadina and Gabriele Ponti for interesting discussions.

REFERENCES

Abramowicz M. A., Czerny B., Lasota J. P., Szuszkiewicz E., 1988, *ApJ*, 332, 646

Artemova I. V., Bisnovatyi-Kogan G. S., Bjoernsson G., Novikov I. D., 1996, *ApJ*, 456, 119

Barrio F. E., Done C., Nayakshin S., 2003, *MNRAS*, 342, 557

Bath G. T., Pringle J. E., 1981, *MNRAS*, 194, 967

Beckmann V., Shrader C. R., Gehrels N., Soldi S., Lubiński P., Zdziarski A. A., Petrucci P.-O., Malzac J., 2005, *ApJ*, 634, 939

Begelman M. C., McKee C. F., 1990, *ApJ*, 358, 375

Belloni T., 2004, *Nuclear Physics B Proceedings Supplements*, 132, 337

Blandford R. D., Begelman M. C., 1999, *MNRAS*, 303, L1

Davis S. W., Blaes O. M., Hubeny I., Turner N. J., 2005, *ApJ*, 621, 372

Davis S. W., Hubeny I., 2006, *ApJS*, 164, 530

Done C., Gierliński M., 2006, *MNRAS*, 367, 659

Draine B. T., Giuliani Jr. J. L., 1984, *ApJ*, 281, 690

Dullemond C. P., 1999, *A&A*, 341, 936

Eardley D. M., Lightman A. P., Shapiro S. L., 1975, *ApJ*, 199, L153

Esin A. A., McClintock J. E., Narayan R., 1997, *ApJ*, 489, 865

Fender R. P., Belloni T. M., Gallo E., 2004, *MNRAS*, 355, 1105

Field G. B., 1965, *ApJ*, 142, 531

Grevesse N., Noels A., 1993, in Pratzo M., Vangioni-Flam E., Casse M., eds, *Origin and Evolution of the Elements Solar composition*. Cambridge University Press, p. 15

Gruzinov A. V., 1998, *ApJ*, 501, 787

Haardt F., Maraschi L., 1991, *ApJ*, 380, L51

Haardt F., Maraschi L., 1993, *ApJ*, 413, 507

Homan J., Wijnands R., van der Klis M., Belloni T., van Paradijs J., Klein-Wolt M., Fender R., Méndez M., 2001, *ApJS*, 132, 377

Ichimaru S., 1977, *ApJ*, 214, 840

Iglesias C. A., Rogers F. J., 1996, *ApJ*, 464, 943

Kubota A., Done C., 2004, *MNRAS*, 353, 980

Lightman A. P., Eardley D. M., 1974, *ApJ*, 187, L1

Mayer M., 2007, *A&A*, 461, 381

Mayer M., Pringle J. E., 2006, *MNRAS*, 368, 379

McClintock J., Remillard R., 2004, in Lewin W., van der Klis M., eds, *Compact Stellar X-ray Sources Black hole binaries*. Cambridge University Press

Meyer F., Meyer-Hofmeister E., 1994, *A&A*, 288, 175

Nakamura K., Osaki Y., 1993, *PASJ*, 45, 775

Narayan R., Yi I., 1995, *ApJ*, 452, 710

Ponti G., Miniutti G., Cappi M., Maraschi L., Fabian A. C., Iwasawa K., 2006, *MNRAS*, 368, 903

Pringle J. E., 1981, *ARA&A*, 19, 137

Ptak A., Terashima Y., Ho L. C., Quataert E., 2004, *ApJ*, 606, 173

Quataert E., 1998, *ApJ*, 500, 978

Quataert E., Gruzinov A., 1999, *ApJ*, 520, 248

Remillard R. A., McClintock J. E., 2006, *ARA&A*, 44, 49

Reynolds C. S., Wilms J., 2000, *ApJ*, 533, 821

Rogers F. J., Iglesias C. A., 1992, *ApJ*, 401, 361

Rózańska A., Czerny B., 2000a, *MNRAS*, 316, 473

Rózańska A., Czerny B., 2000b, *A&A*, 360, 1170

Rybicki G. B., Lightman A. P., 1979, *Radiative processes in astrophysics*. New York, Wiley-Interscience, 1979. 393 p.

Shakura N. I., Sunyaev R. A., 1973, *A&A*, 24, 337

Shapiro S. L., Lightman A. P., Eardley D. M., 1976, *ApJ*, 204, 187

Starling R. L. C., Page M. J., Branduardi-Raymont G., Breeveld A. A., Soria R., Wu K., 2005, *Ap&SS*, 300, 81

Stepney S., Guilbert P. W., 1983, *MNRAS*, 204, 1269

Sutherland R. S., Dopita M. A., 1993, *ApJS*, 88, 253

Svensson R., 1982, *ApJ*, 258, 335

Wandel A., Liang E. P., 1991, *ApJ*, 380, 84

Wandel A., Urry C. M., 1991, *ApJ*, 367, 78

Witt H. J., Czerny B., Zycki P. T., 1997, *MNRAS*, 286, 848

Zhang F., Wu X.-B., 2006, *Chinese Journal of Astronomy and Astrophysics*, 6, 165

Zycki P. T., Collin-Souffrin S., Czerny B., 1995, MNRAS, 277,
70

APPENDIX A: TRANSFORMATIONS

We define the specific energy per unit mass for the disc as

$$e_d = \frac{3}{2} \frac{kT_d}{\mu m_p} + \frac{4\sigma}{c\rho_d} T_d^4, \quad (A1)$$

and the corresponding energy for the corona

$$e_c = \frac{3}{2} \frac{k(T_{p,c} + T_{e,c})}{2\mu m_p}. \quad (A2)$$

Then, with the use of eqns. (1), (2), (8), (9) and the boundary condition (16) we can solve for ρ_c and ρ_d , the densities in the corona and disc and the temperature T_d for given e_d , e_c , $\Sigma_d = \rho_d H_d$ and $\Sigma_c = \rho_c H_c$. We arrive at a system of equations comprising of (A1) and

$$\frac{2}{3} e_c - \Omega^2 \frac{\Sigma_c}{\rho_c} \left(\frac{\Sigma_d}{\rho_d} + \frac{1}{2} \frac{\Sigma_c}{\rho_c} \right) = 0 \quad (A3)$$

$$\rho_d \frac{kT_d}{\mu m_p} + \frac{4\sigma}{3c} T_d^4 - \left(\frac{2}{3} \rho_c e_c + \frac{1}{2} \Omega^2 \frac{\Sigma_d^2}{\rho_d} \right) = 0. \quad (A4)$$

The electron and proton temperature in the corona follow trivially from the specific energy of the electrons and protons (see eq. A2). The variation of H_d and H_c in terms of the internal energies e_d and e_c and surface densities Σ_d and Σ_c is given by

$$\frac{dH_d}{H_d} = \left(\frac{8 - 10\beta_p + 3\beta_p^2}{8 - 7\beta_p} \frac{de_d}{e_d} - \frac{P_c}{2P_d} \frac{H_c}{H_c + H_d} \frac{de_c}{e_c} - \left(1 - \frac{P_c}{P_d} + \frac{\beta_p^2 + 6\beta_p - 8}{8 - 7\beta_p} \right) \frac{d\Sigma_d}{\Sigma_d} - \frac{P_c}{P_d} \frac{d\Sigma_c}{\Sigma_c} \right) / \left(1 - \frac{P_c}{P_d} \frac{H_c}{H_c + H_d} + \frac{8 - 6\beta_p - \beta_p^2}{8 - 7\beta_p} \right) \quad (A5)$$

and

$$\frac{dH_c}{H_c} = \frac{H_c + 2H_d}{2(H_c + H_d)} \frac{de_c}{e_c} - \frac{H_d}{H_d + H_c} \frac{dH_d}{H_d}. \quad (A6)$$

APPENDIX B: THERMAL CONDUCTION

Thermal conduction occurs in media with a temperature gradient. Conduction induces an heat flow to cancel this temperature gradient. In a plasma, electron-proton collision occur typically after the particles travelled the Debye length. The Debye length λ_D is given by

$$\lambda_D = \left(\frac{4\pi\epsilon_0}{e^2} \right)^2 \frac{(mu^2)^2}{2\pi n \ln \Lambda}, \quad (B1)$$

where ϵ_0 is the dielectric constant, e the elementary charge, m the reduced mass (for electron-proton systems it is essentially the electron mass), u the relative speed of electron and proton with respect to each other, n the number density of the plasma and $\ln \Lambda \approx 20$ the Coulomb logarithm.

For a thermal plasma, the average Debye length can be found by integrating over the corresponding isotropic Boltzmann distributions for electrons and protons, respectively. Thus

$$\lambda_D = \left(\frac{4\pi\epsilon_0}{e^2} \right)^2 \frac{9k_B^2 T_e^2}{2\pi n \ln \Lambda} \left(1 + \frac{m_e}{m_p} \frac{T_p}{T_e} \right)^2, \quad (B2)$$

where T_e and T_p is the temperature of the electrons and protons and k_B is the Boltzmann constant. Since both the electrons and protons have an isotropic velocity distribution, the effects of alignment and anti-alignment cancel and we do not need to treat any angle-dependent terms in the velocity u^2 . For further reference we define

$$\xi_{ep} = \frac{m_e}{m_p} \frac{T_p}{T_e}. \quad (B3)$$

Note that for a one-temperature plasma ($T_e = T_p$) the correction factor $1 + \xi_{ep}$ is close to unity and the classical Debye length is reproduced.

The conductive flux of heat then can be described as the thermal average of $nmu^2\lambda_D(\partial v/\partial x)$. We find

$$\begin{aligned} q_{\text{cond}} &= \left\langle n m_e u^2 \lambda_D \frac{\partial u}{\partial x} \right\rangle_{\text{th}} \\ &= \frac{1}{2} \left\langle n m_e u \lambda_D \left(\frac{\partial u_e^2}{\partial x} + \frac{\partial u_p^2}{\partial x} \right) \right\rangle_{\text{th}} \\ &\approx \frac{1}{2} n \lambda_D \sqrt{\frac{kT_e}{m_e}} \sqrt{1 + \xi_{ep}} \left(\frac{\partial (kT_e)}{\partial x} + \frac{m_e}{m_p} \frac{\partial (kT_p)}{\partial x} \right), \end{aligned}$$

where u_e and u_p are the respective speeds of the electrons and protons. Together with the Debye length (B2) we find

$$q_{\text{cond}} = \underbrace{\left(\frac{4\pi\epsilon_0}{e^2} \right)^2 \frac{9k(k_B T_e)^{\frac{5}{2}} (1 + \xi_{ep})^{\frac{5}{2}}}{4\pi\sqrt{m_e} \ln \Lambda}}_{\kappa_{\text{cond}}} \left(\frac{\partial T_e}{\partial x} + \frac{m_e}{m_p} \frac{\partial T_p}{\partial x} \right). \quad (\text{B4})$$

Note that we again find for a one-temperature plasma ($T_e = T_p$) the correction factor $1 + \xi_{ep}$ is close to unity and moreover the electron and proton temperature gradient are the same and hence the proton temperature gradient contributions to the conductive flux can be neglected. The value of the parameter κ_{cond} is

$$\kappa_{\text{cond}} = 6.9 \cdot 10^{-7} T_e^{\frac{5}{2}} (1 + \xi_{ep})^{\frac{5}{2}} \text{ erg s}^{-1} \text{cm}^{-1} \text{K}^{-1}. \quad (\text{B5})$$

This is somewhat larger than the value quoted in Begelman & McKee (1990). Their value (not containing the correction factor $1 + \xi_{ep}$) is based on Draine & Giuliani (1984) who use a higher value for the Coulomb logarithm and furthermore include effects of different ion species. Our value however is only about 20 per cent larger. Compared with the other approximations in the model presented in this paper we consider our value to be sufficiently accurate.

The physical effect presented in this section is similar to Mayer (2007). In both calculations the classical derivations are extended for a two-temperature plasma. Then the proton contributions cannot be neglected any more since their plasma speed can become comparable to the electron plasma speed.